Proton and Ion Linear Accelerators

Yuri Batygin,[1] Sergey Kurennoy,[1] Dmitry Gorelov,[1] Vyacheslav Yakovlev [2], Tyler Fronk[3]

[1]Los Alamos National Laboratory
[2]Fermi National Accelerator Laboratory
[3]Sandia National Laboratories

U.S. Particle Accelerator School

June 7 – July 2, 2021

Proton and Ion Linear Accelerators

13. RF accelerating structures, Lecture 5

Vyacheslav Yakovlev, Fermilab

U.S. Particle Accelerator School (USPAS)

Education in Beam Physics and Accelerator Technology

June 25, 2021

RF accelerating structures

Outline:

- Architecture of modern SRF proton accelerators;
- SRF around the world
- Επιλογος
- Home tasks.
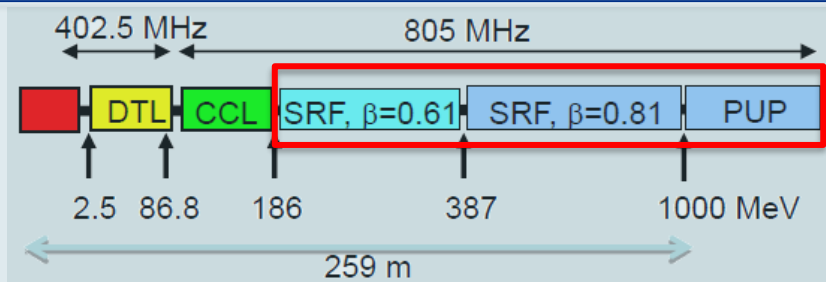
🎷 **Fermilab**

Chapter 9.

Architecture of SRF accelerators.

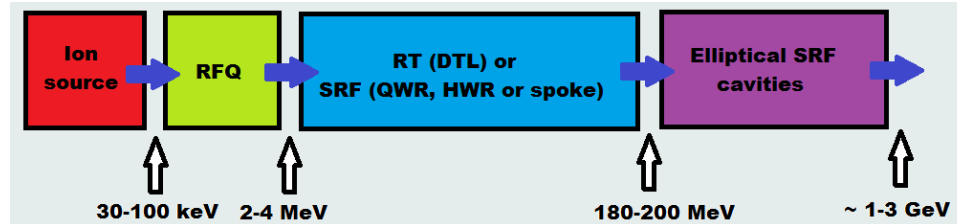**a. proton/ion SRF linacs:**
- RT or SRF front end?
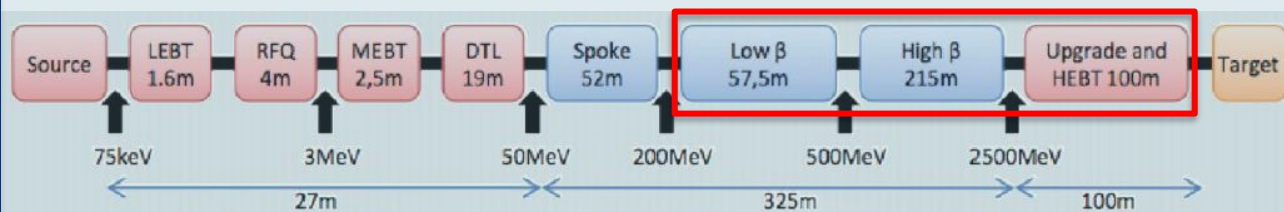- choice of beamline elements;
- lattice design.

b. electron SRF linacs.

🔷 **Fermilab**
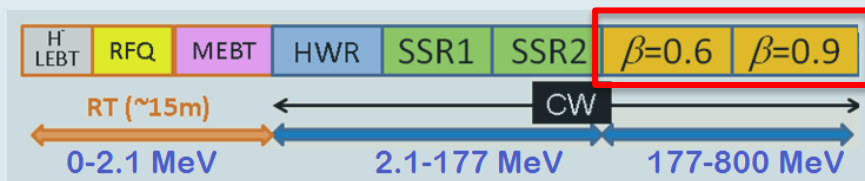
Architecture of a GeV–range proton SRF accelerator:
Layout of typical modern proton SRF accelerator.

SNS (ORNL): H⁻ ,1 GeV, 6% DF, 1.44 MW to accumulator ring
In operation

ESS (Lund): p⁺, 2.5 GeV, 4% DF, 5 MW to target
Under construction

PIP II (FNAL): H⁻ ,800 MeV, up to 100% DF, up to 1.6 MW
Design

🔶 Fermilab

Linac Design Philosophy:

❑ RT or SRF frontend?

- For low duty factor RT frontend (up to ~200 MeV) may be used
- For high DF or CW SRF is necessary from the beginning

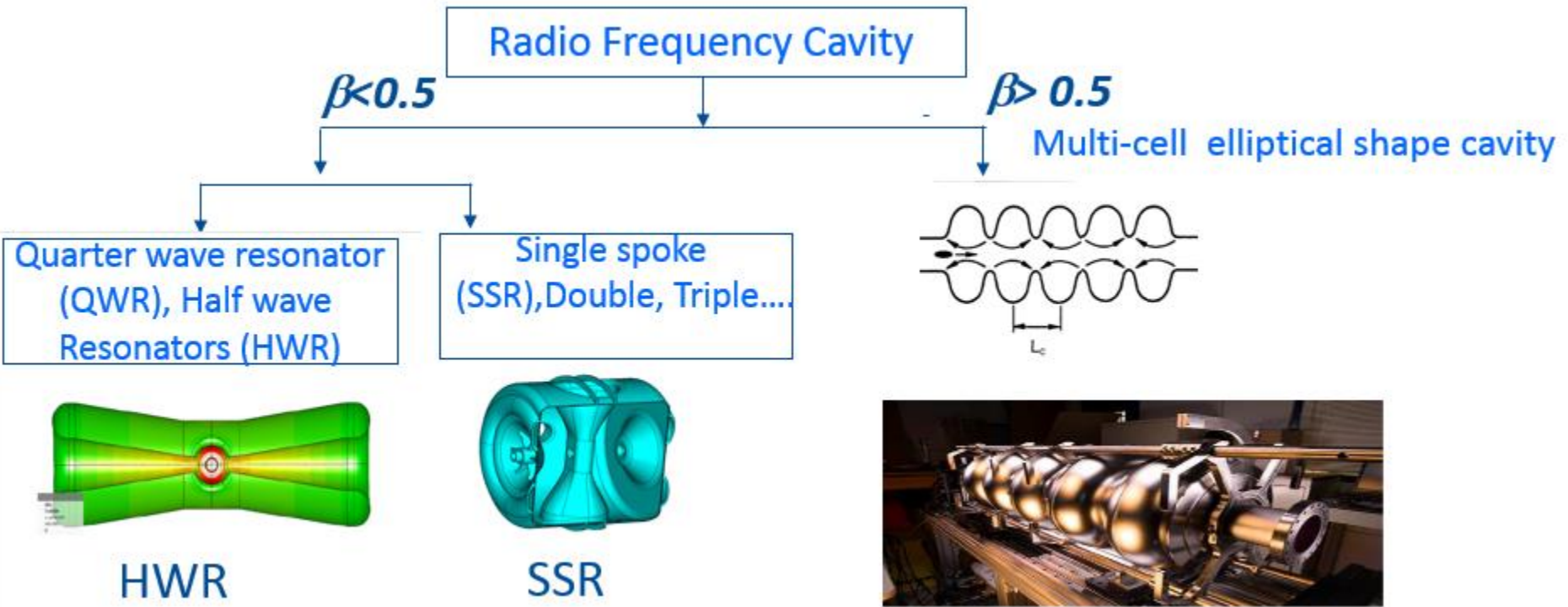❑ Choice of beam line elements

- Accelerating RF Cavities
- Focusing Magnets

❑ Lattice Design

- Focusing Period
- Transition Energy between Sections

🟦 **Fermilab**

RF cavities:

- Lower RF frequency provides better interaction with beam.
- RF defocusing factor is inversely proportional to frequency.
- Lower frequency implies larger RF bucket and hence larger longitudinal acceptance.

🔷 Fermilab

RF cavities:

❑ The frequency choices for multi-cell:

- Cavity length is about the same for the same β_G (the same number of couplers, tuners, etc). Typical length ~0.8-1 m depending on β_G (from iris to iris)
- Lower frequencies $\rightarrow$ bigger size, higher cost, more difficult handling, microphonics
  - but: lower losses per unit length (smaller R/Q, but lower R_s); larger aperture (current interception), smaller beam defocusing; smaller number of cells and therefore, smaller a/λ, smaller K_m and K_e and smaller numbers of cavity types.
- Typically , they use 650 – 800 MHz, and 5-7 cells/cavity:
  - SNS: 804 MHz, 6 cells/cavity (in operation)
  - ESS: 704 MHZ, 5 cells/cavity (under construction)
  - PIP II: 650 MHz, 5 cells/cavity (under development)

❑ The frequency choices for the front end:

- Subharmonics of the main frequency.

❑ Acceleration gradient choice (high DF, CW):

- Quench, $B_{peak} \gtrsim$ 70-80 mT
- Field emission, $E_{peak} \gtrsim$ 40 MV/m
- Thermal breakdown typically is not an issue for proton linacs.

🫱 **Fermilab**

RF cavities:

- Selection of the maximum accelerating gradients in cavities are made on the basis of :
    - Peak surface magnetic field
    - Peak surface Electrical field
- Choices of peak magnetic fields are derived from:
    - Dynamics heat load due to accelerating mode
    - Cavity quenching.
- Choices of peak surface field is made to avoid field emission

CW Linac assumptions:
- 162.5 MHz: $H_{pk} < 50mT$
- 325 MHz: $H_{pk} < 60mT$
- 650 MHz: $H_{pk} < 70mT$
- $E_{pk} < 40$ MV/m.

Accelerating Gradient in PIP-II Linac

	HWR	SSR1	SSR2	LB650	HB650
Gradient (MV/m)	9.7	10	11.4	15.9	17.8

🔷 **Fermilab**

Focusing elements:

❖ Normal conducting magnets are cheaper but superconducting magnets are:
  - ➢ Compact in size
  - ➢ Provide intense magnetic field with low power consumption.

❖ Low energy part of SRF linac typically has solenoidal focusing:
  - ❖ Provide radial focusing

❖ Intermediate and high energy section of linac use normal conducting doublet focusing.
  - ❖ Simplify cavity magnetic shielding requirements

❖ Correctors are built in each magnets.

❖ Solenoidal and doublet focussing keeps the beam round in transverse planes.

- • *Focusing magnets in each section*

Section	HWR	SSR1	SSR2	LB650	HB650
Magnet	S	S	S	FD	FD

S – solenoid, FD – doublet (F : focusing and D: Defocusing quadrupole).
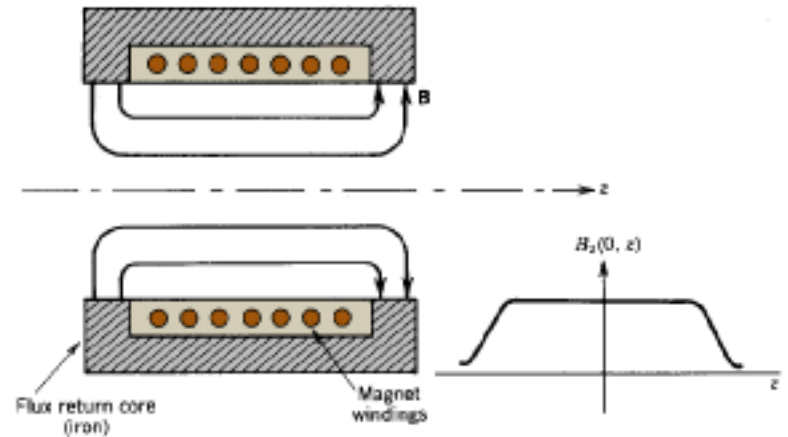
🔷 Fermilab

Focusing elements:

❑ **Solenoid:**

Solenoid focal length f:
(non-relativistic case, T is a particle kinetic energy, $T=mv^2/2$.)

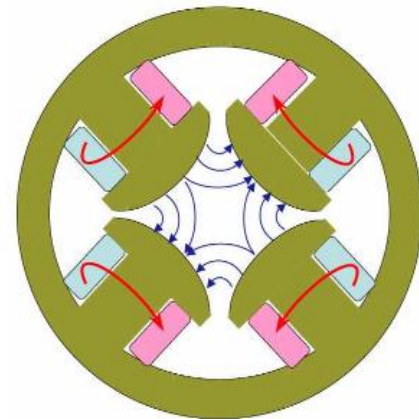$$\frac{1}{f} = \frac{q^2}{8Tm} \int B_z^2 dz$$

- Focal length is proportional to β^2;
- Focal length is inversed proportional to $B_z^2 L$, L is the solenoid length;
- Therefore, solenoid can be used for low β ($\beta<0.5$). For higher β quad is used.

❑ **Quadrupole lens:**

Quad focal length f:

$$\frac{1}{f} = \frac{qB'L}{\gamma\beta mc}$$

🔷 **Fermilab**

Focusing elements:

For low section SC solenoids are used.

- Simple and inexpensive;
- Filed up to 6-8 T;
- SRF cavity should have < 10 mT on the SRF cavity surface:
  remnant solenoid field should be compensated
- Solenoid contains correction coils (steering dipoles)
- Alignment (typically <0.3- 0.5 mm, <5 mrad tilt);
- Quench protection;
- Leads

Magnetic Shield
LHe Vessel
Flux Return
Bandage
Main Coil
Steering Dipoles
Beam Pipe
Bucking Coil

🔷 **Fermilab**
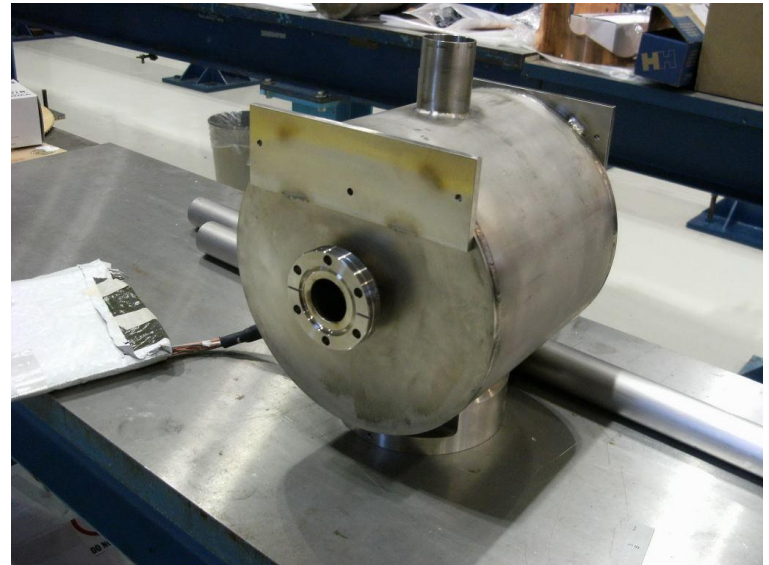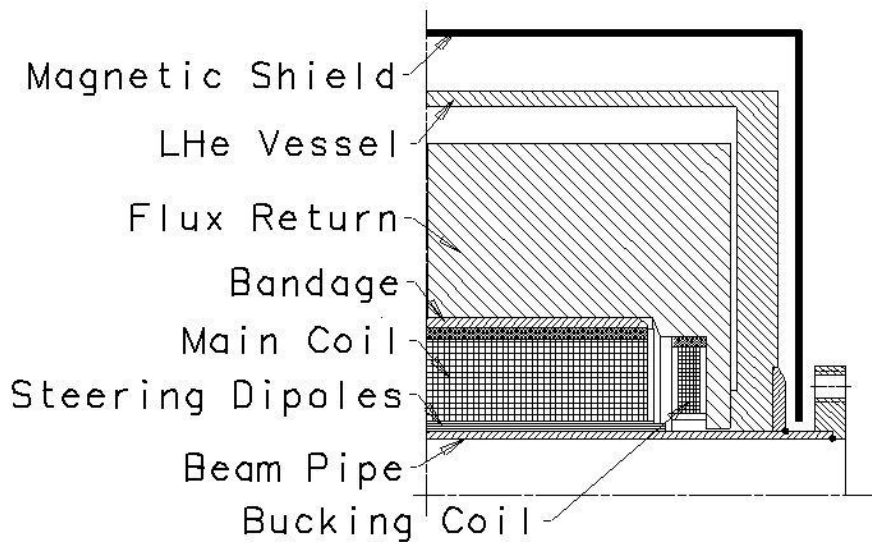
Lattice Design: Focusing Periods

- Length of the focusing period is kept short, especially in the low energy section where beam is non-relativistic and non-linear force may be significant .

Cryomodule Arrangement
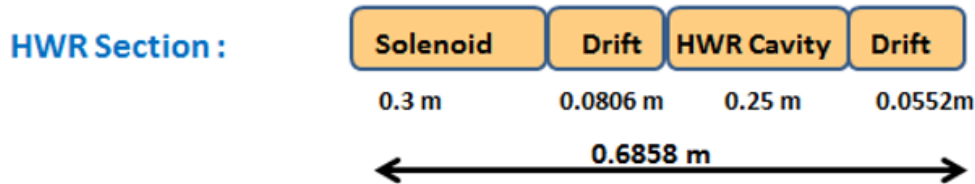
HWR Section :

Solenoid	Drift	HWR Cavity	Drift
0.3 m	0.0806 m	0.25 m	0.0552m

0.6858 m

SC-SC-SC-SC-SC-SC-SC-SC

SSR1 Section :

0.3 m		0.3 m		
SSR1 Cavity		Solenoid	SSR1 Cavity	SSR1 Cavity

0.4 m   0.45 m

1.25 m

CSC-CSC-CSC-CSC

SSR2 Section :

0.32 m		0.4767 m	
Solenoid	Cavity	Cavity	Solenoid

0.75 m   0.75 m

2.25 m

SCC-SCC-SC

🔵 Fermilab
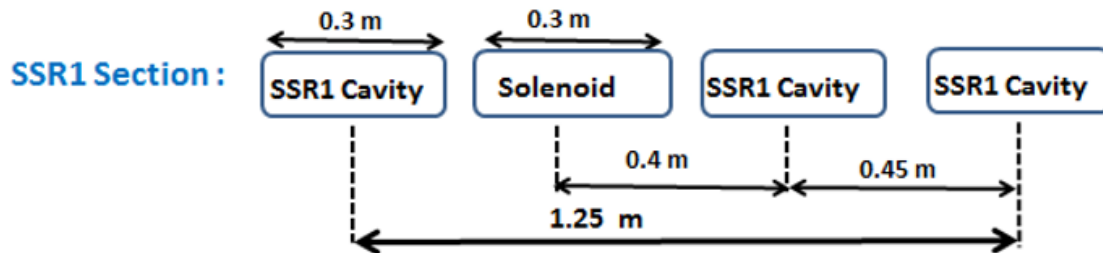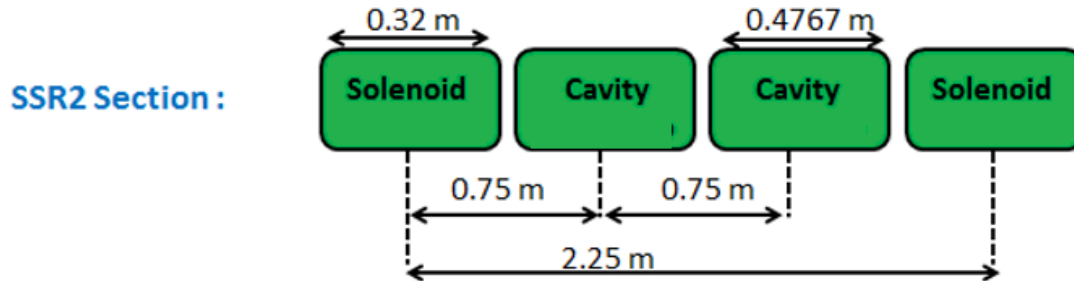
Lattice Design: Focusing Period in High Energy Section

- Frequency jump from 325 MHz to 650 MHz at LB650 MHz section
- Solenoidal focusing is replaced with quadrupole doublet.
- Same family of doublet is used in both LB650 and HB650 sections.

🐝 **Fermilab**

Transition Energy between Sections :

- Transition Energy between Sections (type cavity change). Optimization in order to minimize the number of cavities.
- Beam matching between sections and cryomodules are achieved using elements of each side of transitions. Avoiding abrupt changes in beam envelopes to reduce possibility of halo formations.
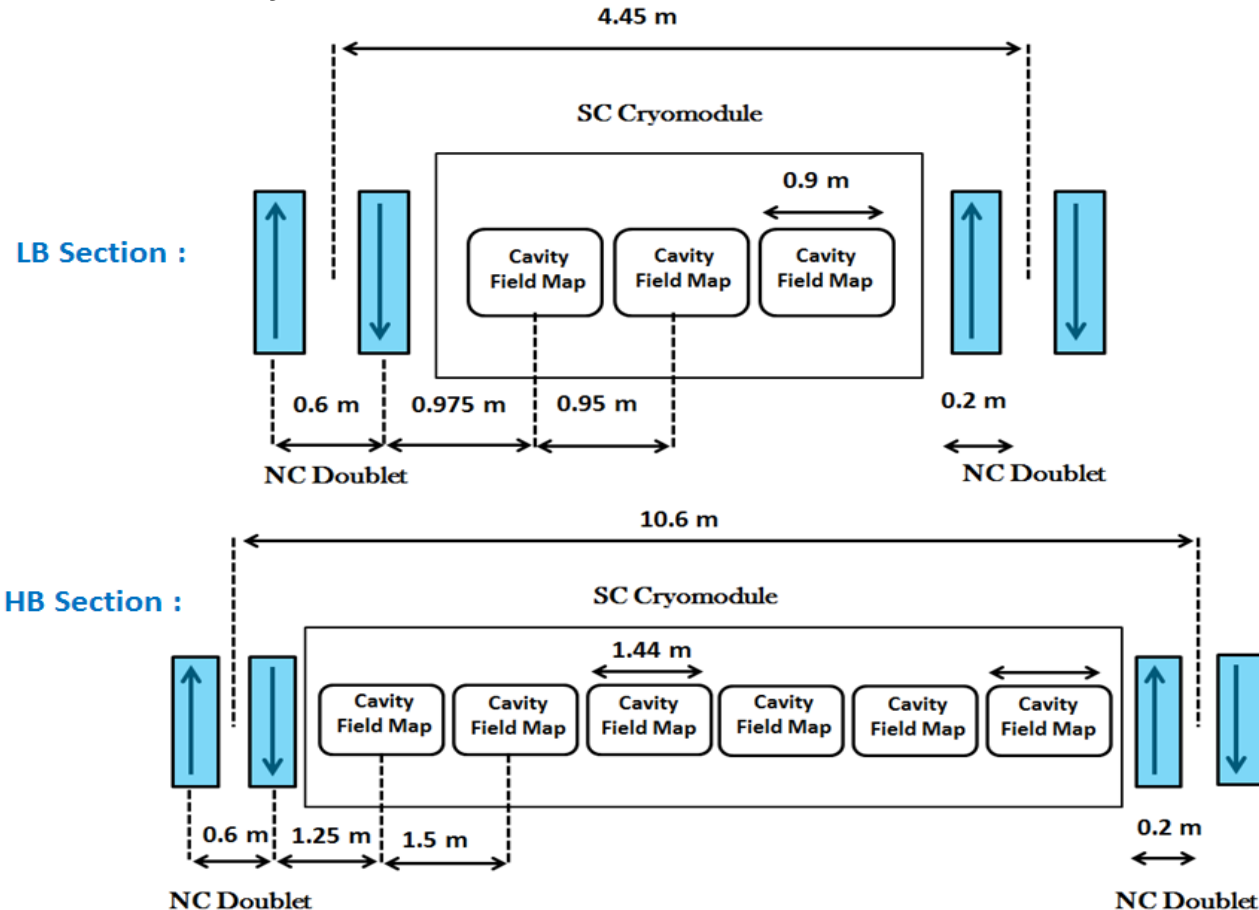- Adiabatic variation in phase advance along linac. Reduces possibility of beam mismatch.
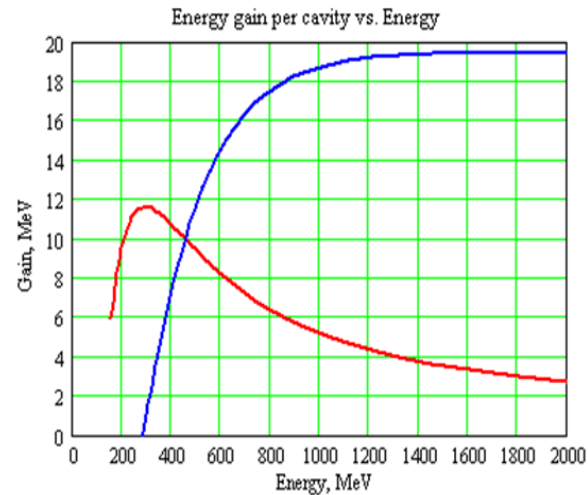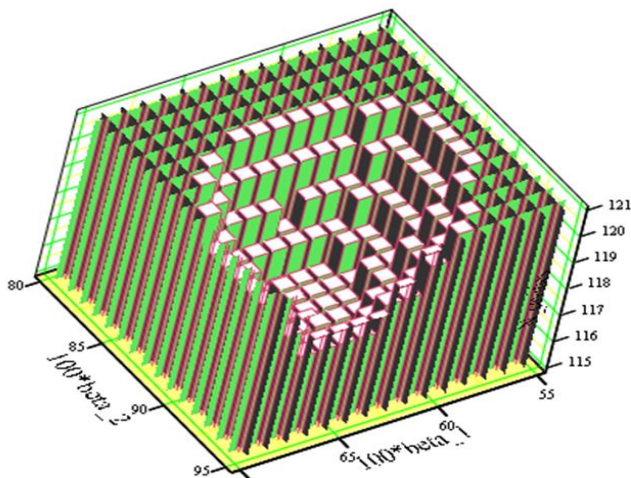
Number of cavities required for acceleration from 185 to 800 MeV versus cavity beta in the LB650 and HB650 sections (left) and the energy gain per cavity versus particle energy (right) for LB650 (red curve) and HB650 (blue curve) cavities.

Architecture of a GeV–range proton SRF accelerator:

Correct selections of transitional energy provide better optimization of real estate gradient and reduction in total number of beam line elements.

Transition time factor v/s beta
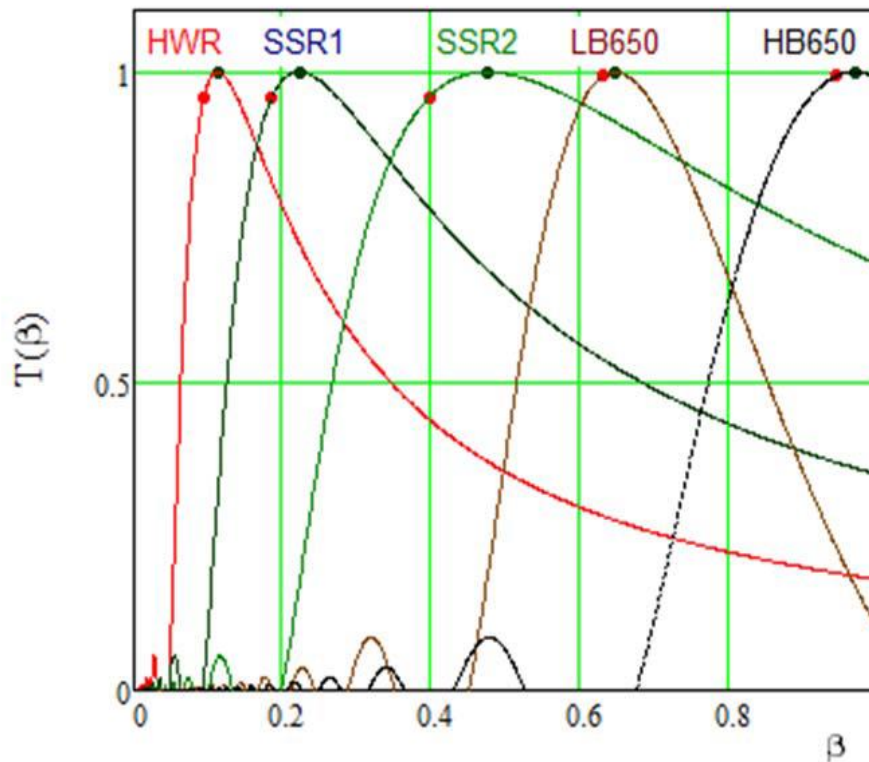
Sections	Initial Energy (MeV)	Design Beta	Beta range
HWR	2.1	0.094	0.067 -0.147
SSR1	10.3	0.186	0.147-0.266
SSR2	35	0.398	0.266-0.55
LB 650	185	0.61	0.55-0.758
HB 650	500	0.92	0.758-0.842

‡ Fermilab

Acceleration voltage distribution

Voltage Amplitude in Cavities
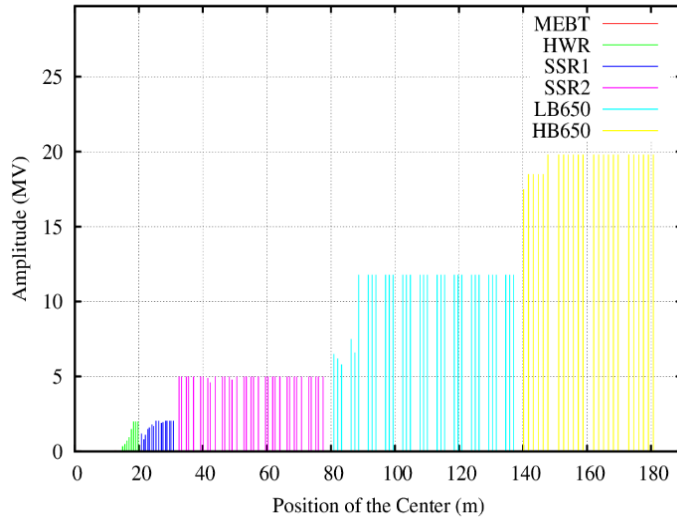
Voltage gain by beam
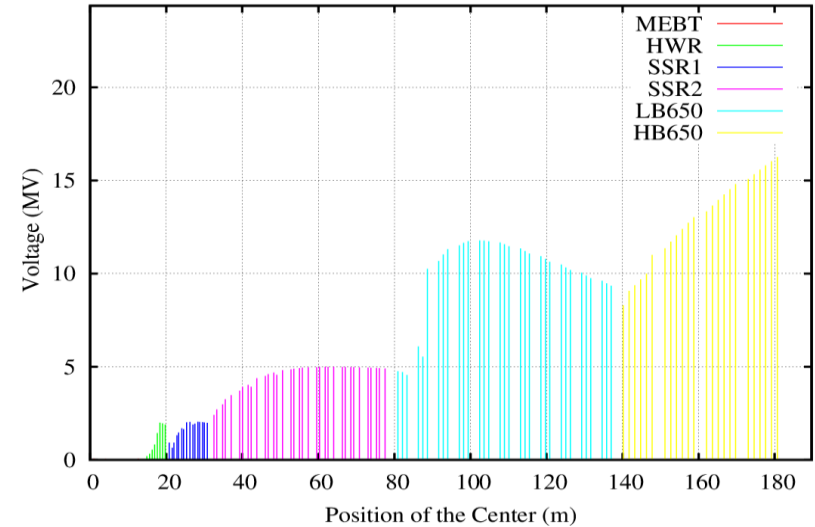
- Maximum Energy gain in PIP-II SC cavities

	HWR	SSR1	SSR2	LB650	HB650
Max. Egain (MeV)	2	2.05	5	11.9	19.9

🔁 Fermilab
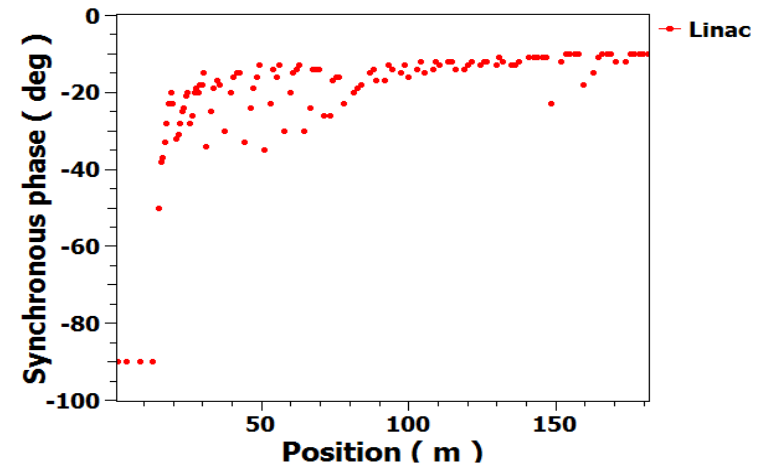
Summary:

❑ Architecture of a big SRF linac is determined by:
- accelerated particles – electrons, protons or ions;
- accelerator operation regime – pulsed or CW;
- accelerator parameters – energy and power.

❑ For a proton accelerator the choice of the front end – RT or SRF – depends on the operation regime, pulsed or CW.

❑ The frequencies and cavity types for a proton or an ion accelerator should be determined;

❑ The types of the focusing elements should be selected.

❑ The lattice should be designed, which provides
- acceleration
- focusing
- bunching.

❑ Break points between the section with different cavity types should be optimized;

❑ The sections should be matched to each other to provide required beam quality.

Chapter 10.

SRF around the world

춘↯ Fermilab

SRF around the world
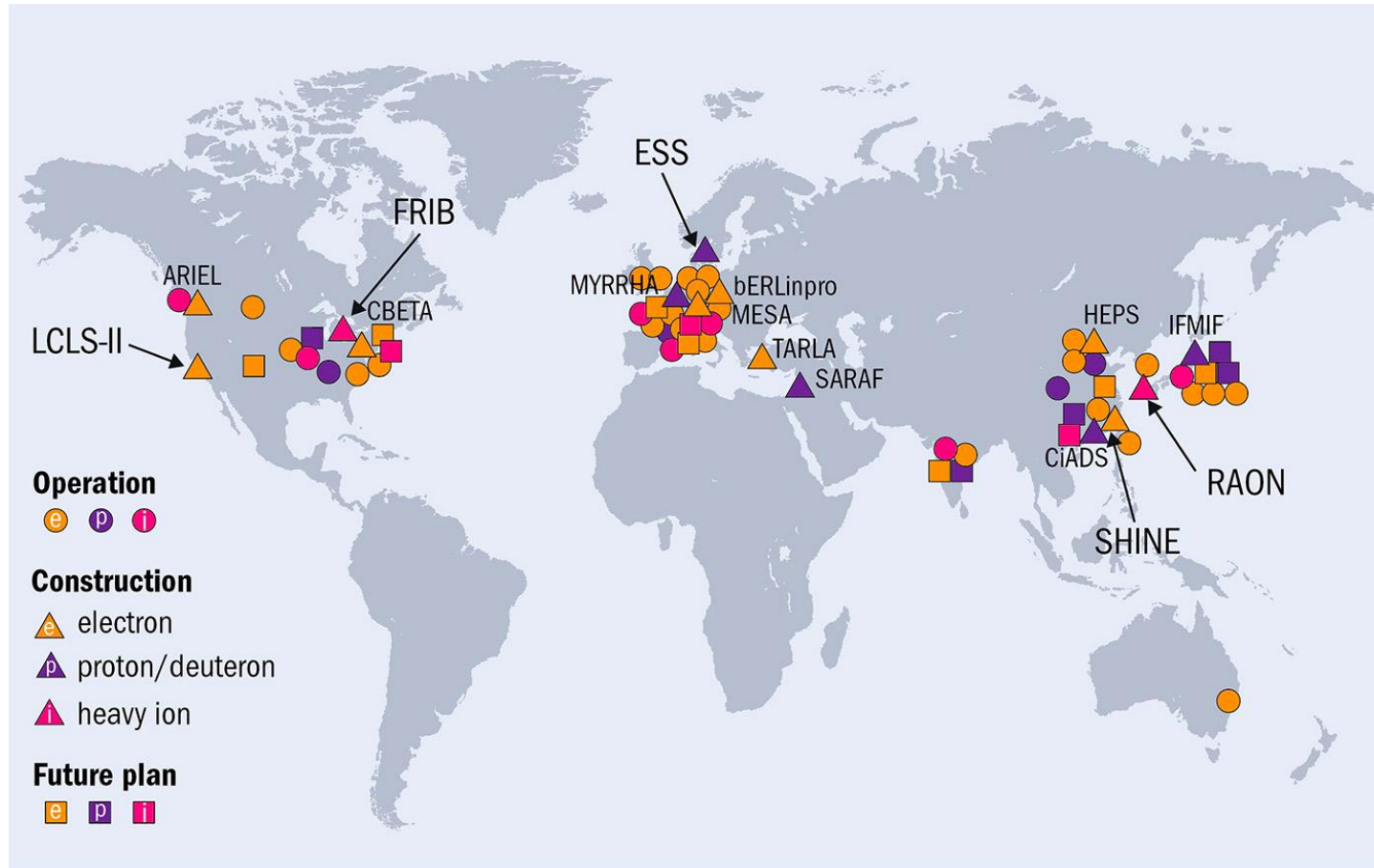
Global view Distribution of superconducting particle accelerators using SRF structures for electrons (orange), protons (purple) and heavy ions (pink). More than 30 SRF accelerators are in operation (circles), approximately 15 are presently under construction (triangles) and more than 10 future projects are under consideration (squares). *Credit: CERN*

🐝 Fermilab

Big SRF Accelerator Facilities:

Linac	Laboratory	Application	Acc. Particle	Operation	Status
SNS	ORNL, USA	Neutron Source	H$^-$	pulsed	Operation
ESS	ESS, Sweden	Neutron Source	p	pulsed	Construction
CIADS	IMP, China	ADS	p	CW	R&D
ISNS	Indore, India	Neutron Source	p	pulsed	R&D
ADSS	BARC, India	ADS	p	CW	R&D
PIP II	FNAL, USA	Neutrino/Muons	H$^-$	CW/pulsed	R&D
FRIB	MSU, USA	Nucellar physics	Ions	CW	Commissioning
RAON	RISP, S.Korea	Nucellar physics	Ions	CW	Construction
CEBAF	JLAB, USA	Nucellar physics	e$^-$	CW	Operation
XFEL	DESY, Germany	FEL	e$^-$	pulsed	Operation
SHINE	SINAP, China	FEL	e$^-$	CW	Construction
LCLS II	SLAC, USA	FEL	e$^-$	CW	Construction

🟂 Fermilab

New large SRF accelerator installations

CEBAF Upgrade - JLAB Upgrade 6.5 GeV => 12 GeV electrons	80 cavities	**Electrons**
XFEL – Hamburg, Germany 17.5 GeV electrons – Pulsed X-ray FEL	840 cavities	
LCLS-II (+ LCLS-II-HE) – SLAC 4 GeV electrons – CW X-ray FEL	296 (+184) cavities	
SPIRAL-II – France 30 MeV, 5 mA protons -> Heavy Ions	28 cavities	**Ions**
FRIB – MSU 500 kW, heavy ion beams for nuclear astrophysics	340 cavities	
ESS – Sweden 1 – 2 GeV, 5 MW Pulsed spallation source	150 cavities	**Protons**
PIP-II – Fermilab 800 MV High intensity proton linac for neutrino beams	115 cavities	

Coming up: *SHINE* in China, *EIC* at BNL, *ILC* in Japan, *FCC-ee/FCC-hh* at CERN, *CEPC-SPPC* in China, *Accelerator complex upgrade to 2.4 MW* at Fermilab

🎇 **Fermilab**

SRF gradient achievements and applications

Gradient growth SRF linac accelerating gradient achievements and application specifications since 1970.

CW SRF Linacs – SCA: Stanford Superconducting Accelerator; MUSL: llinois Microtron Using a Superconducting Linac; CEBAF: Continuous Electron Beam Accelerator Facility; JLab FEL: JLab Free Electron Laser; ELBE: HZDR Electron Linear accelerator with high Brillance and Low Emittance; ALICE: STFC Accelerators and Lasers In Combined Experiments; ARIEL: TRIUMF Advanced Rare IsotopE Laboratory; LCLS-II:

Linac Coherence Light Source extension; SHINE: Shanghai High Brightness Photon Facility.

Pulsed SRF Linacs – FAST: Fermilab Accelerator Science and Technology Facility; STF: KEK Superconducting RF Test Facility; E-XFEL: European Xray Free Electron Laser; ILC: International Linear Collider.
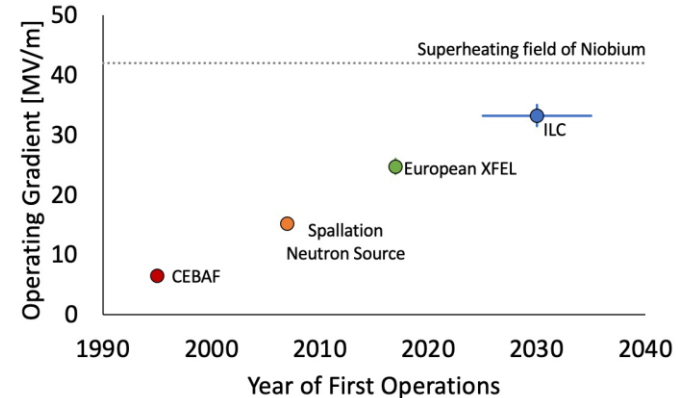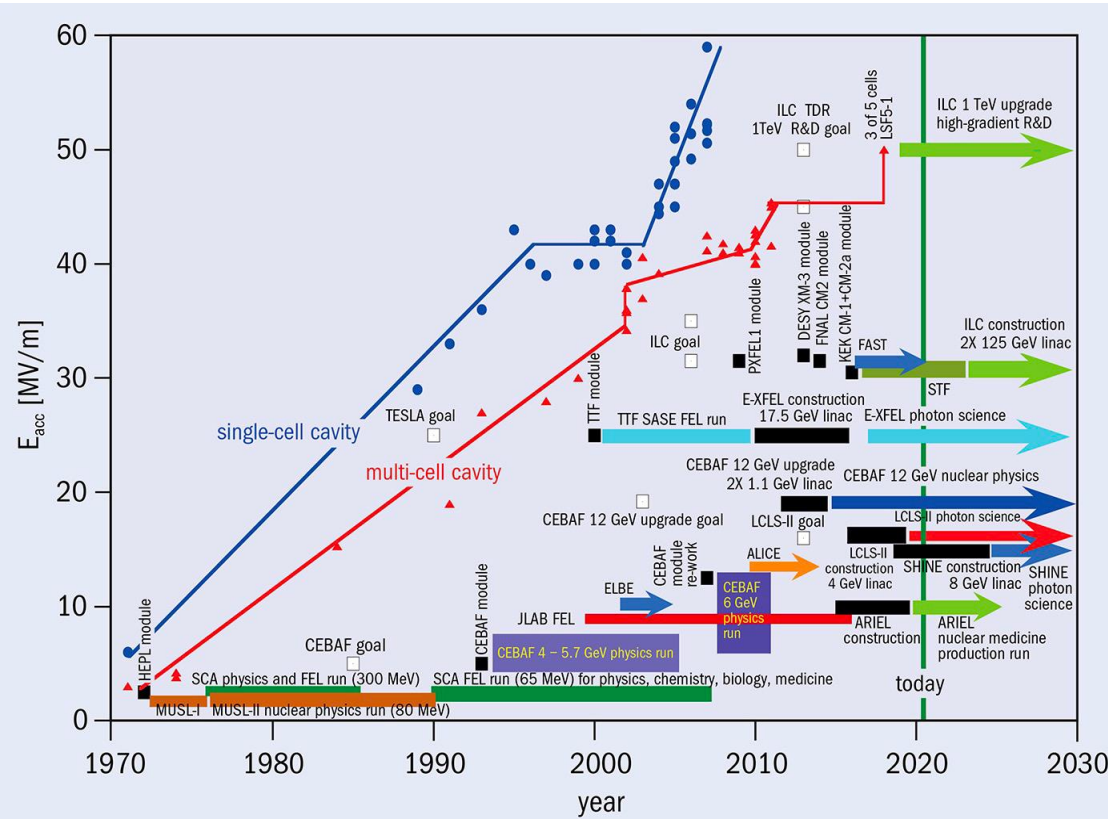
Credit: Source: R Geng/ORNL

🎷 **Fermilab**

Fermilab PIP-II

IS	LEBT	RFQ	MEBT	β=0.11	β=0.22	β=0.51	β=0.61	β=0.9

RT   SC

162.5 MHz   325 MHz   650 MHz
0.03-11 MeV   11-177 MeV   177-800 MeV

(115 Cavities)

Half Wave

Spokes

Medium-Beta Elliptical Cavities

High-Beta Elliptical Cavities

Architecture of Facility for Rare Isotope Beams (FRIB, MSU)

Beam Delivery System To Target

β=0.085 Matching Cryomodule
β=0.29 Matching Cryomodule
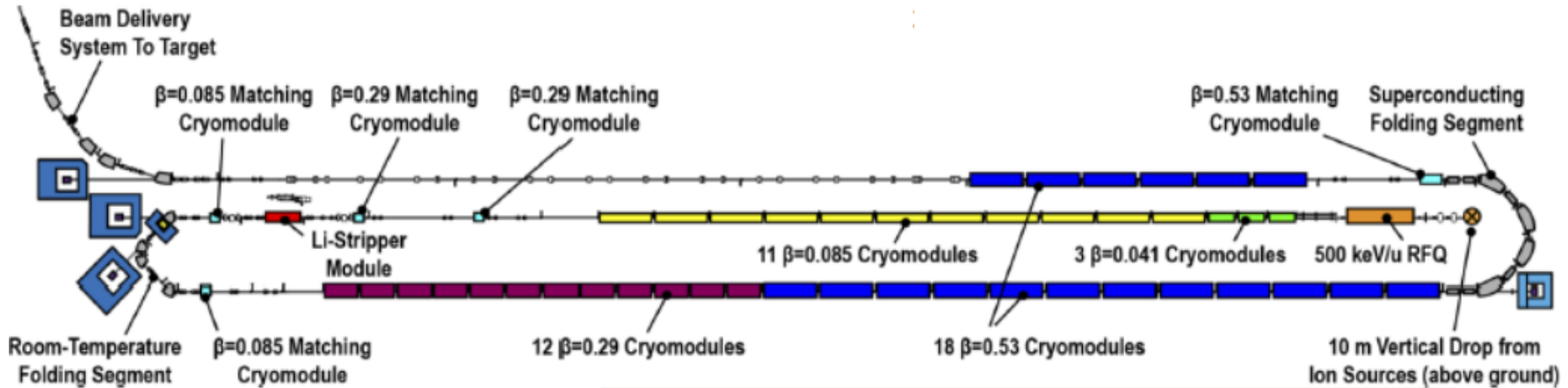β=0.29 Matching Cryomodule
β=0.53 Matching Cryomodule
Superconducting Folding Segment

Li-Stripper Module

11 β=0.085 Cryomodules
3 β=0.041 Cryomodules
500 keV/u RFQ

Room-Temperature Folding Segment
β=0.085 Matching Cryomodule
12 β=0.29 Cryomodules
18 β=0.53 Cryomodules
10 m Vertical Drop from Ion Sources (above ground)

K. Saito, September 2014 LINAC14 THIOA02

FRIB cavities

1- meter
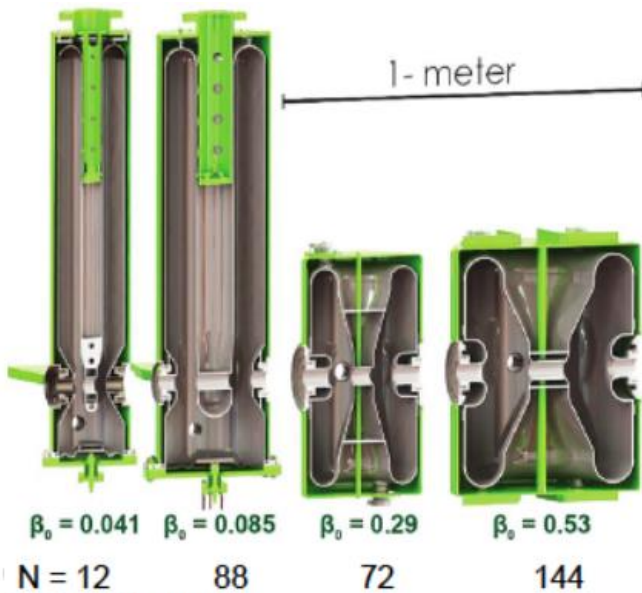
β₀ = 0.041   β₀ = 0.085   β₀ = 0.29   β₀ = 0.53
N = 12   88   72   144
316 cavities need,
total 347 including matching module, spares

Cavity Type	QWR	QWR	HWR	HWR
β_0	0.041	0.085	0.285	0.53
f [MHz]	80.5	80.5	322	322
V_a [MV]	0.810	1.80	2.09	3.70
E_{acc} [MV/m]	5.29	5.68	7.89	7.51
E_p/E_{acc}	5.82	5.89	4.22	3.53
B_p/E_{acc} [mT/(MV/m)]	10.3	12.1	7.55	8.41
R/Q [Ω]	402	455	224	230
G [Ω]	15.3	22.3	77.9	107
Aperture [m]	0.036	0.036	0.040	0.040
$L_{eff} \equiv \beta\lambda$ [m]	0.153	0.317	0.265	0.493
Lorenz detuning [Hz/(MV/m)²]	< 4	< 4	< 4	< 4
Specific Q_0@VT	1.4E+9	2.0E+9	5.5e+9	9.2E+9
Q_L	6.3E+6	1.9E+6	5.6E+6	9.7E+6

🔷 Fermilab

FRIB linac is successfully commissioned in May 2021!
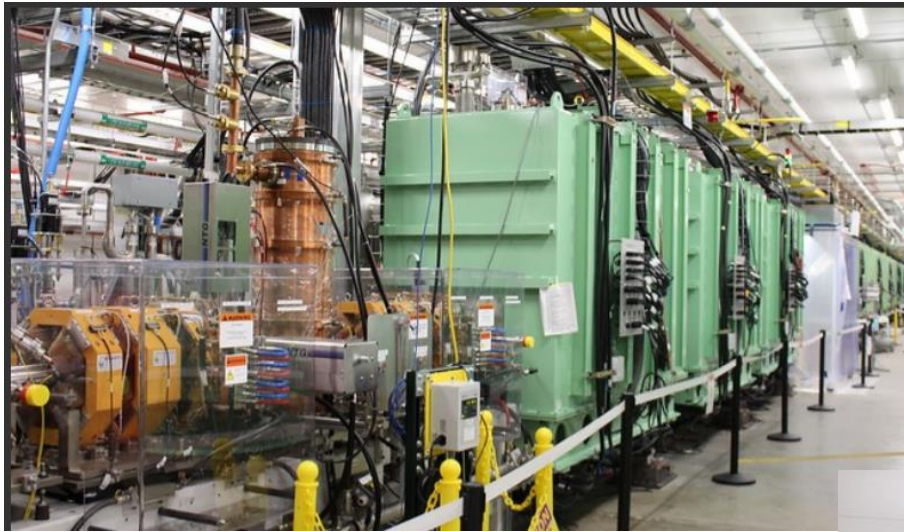
5-cell 644 MHz cavities for FRIB upgrade

‡Fermilab

Architecture of LCLS II (electron SRF Linac for FEL)

	L0	L1		L2	L3	
	$\varphi =$ **	$\varphi = -21°$	HL	$\varphi = -21°$	$\varphi = 0$	
	V_0 =94 MV	V_0 =223 MV	$\varphi = -165°$	V_0 =1447 MV	V_0 =2409 MV	
	I_{pk} = 12 A	I_{pk} = 12 A	V_0 =55 MV	I_{pk} = 50 A	I_{pk} = 1.0 kA	
	L_b = 2.0 mm	L_b =2.0 mm		L_b = 0.56 mm	L_b = 0.024 mm	

CM01 — CM2,3 — 3.9GHz — CM04 ··· CM15 — CM16 ··· CM35 — LTU

GUN — LH — BC1 — 12 CMs — BC2 — 20 CMs

GUN 0.75 MeV

LH
E = 95 MeV
R_{56} = -14.5 mm
σ_δ = 0.05 %

BC1
E = 250 MeV
R_{56} = -55 mm
σ_δ = 1.4 %

BC2
E = 1600 MeV
R_{56} = -60 mm
σ_δ = 0.46 %

LTU
E = 4.0 GeV
R_{56} = 0
$\sigma_\delta \approx$ 0.016%
2-km

100-pC machine layout: Oct. 8, 2013; v21 ASTRA run; Bunch length L_b is FWHM

Fermilab

European XFEL

View Along the 1 km Long Superconducting Accelerator

- EXFEL is the world largest SRF application at 17.5 GeV (800 cavities).
- Operating gradient is 23.5 MV/m.
- Construction is complete, commissioning has started.
- First lasing in May 2017!

IPAC '17, 15.5.2017
Winni Decking, DESY

🎇 Fermilab

Επιλογος

❖ SRF Liner Accelerator is self-consistent system, parts of it strongly depend on each other. Deep understanding and careful analysis of subsystems and components as well as their interaction are necessary to achieve required beam parameters and facility reliability at minimal capital and operation cost.

❖ The design process will never be reduced to just a few simple rules or recipes. Using an existing design as a base for developing a new system is OK and can shorten the new system development time, but the system designers should be aware that even seemingly small changes could bring big consequences.

❖ As accelerator application demands continue to increase (higher energy, higher luminosity, brighter beams, more efficient accelerators, …) there will be no shortage of new challenges to tackle in the future.

❖ The field of RF superconductivity is very active. The SRF technology is the technology of choice for many types of accelerators.

🔷 Fermilab

There will always be ample opportunities for imagination, originality, and common sense.

🎇 **Fermilab**

The end

Tasks for Homework

Homework

Task 1. Lecture

SRF 5-cell cavity designed for PIP II has the following parameters:

- Operating frequency is 650 MHz
- Acceleration voltage V is 20 MV
- R/Q is 620 Ohm
- Q_0 at operation voltage is 3e10
- The beam current I is 2 mA

Estimate for CW operation:

- The cavity loaded quality factor, $Q_L = V/(I\cdot(R/Q))$
- The cavity time constant, $\tau = 2Q_L/\omega$.
- The cavity bandwidth , $\delta f = f/Q_L$;
- Loss power in the cavity walls;
- The power transferred to the beam;
- Power required for refrigeration; take **C**oefficient **o**f **P**erformance CoP= 1.e3 W/W, i.e., in order to remove 1 W from the cavity wall one needs wall plug power of 1 kW);
- Acceleration efficiency, the beam power over the sum of the RF power and power required for refrigeration.

🌠 **Fermilab**

Homework

Task 2.

PIP II SRF accelerator has CW capability, but will operate in the pulsed mode as an injector to the booster ring. The beam and cavity parameters are the same as for CW, Task 1. The beam pulse t_{beam} is 0.55 msec, repletion rate is 20 Hz. The beam appears when the cavity voltage reaches the operating value V, and backward wave (from the cavity to the RF source) is zero. Note that this wave is a sum of the reflection from the coupling element (which is equal to the incident wave), and the wave radiated from the cavity to the line. In the beginning of the cavity filling, the radiation is zero (the cavity is empty), and the backward wave is equal to reflection from the coupling element, and thus, to the incident wave. If there is no beam, the backward wave is again equal to the incident wave (no losses in the cavity) after the voltage reaches its maximal value, but it is again the sum of the wave reflected from the coupling element and radiated wave. It can be only if the radiated wave is two times larger than the wave reflected from the coupling element, and has opposite sign. It means that the beam appears when the cavity field reaches half of the maximal value (zero backward wave, the reflected wave is equal to the radiated wave, and they compensate each other). The cavity voltage, thus, increases during the filling   as $V(t) = 2V(1-\exp(-t/\tau))$, τ is the time constant, $\tau = 2Q_L/\omega$. Filling is over when $V(t_{fill}) = V$, and therefore, the filling time t_{fill} is equal to $\tau \cdot \ln 2$. After the beam ends, the RF source is turned off, and cavity discharges as $V(t) = V\exp(-t/\tau)$. Thus, the cavity voltage has the following behavior:
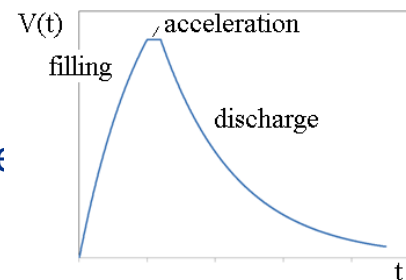
Homework

Task 2 (cont.)

- $V(t) = 2V(1-exp(-t/\tau))$, $t < t_{fill} = \tau \cdot ln2$ - filling; RF is on, no beam;
- $V(t) = V$, the beam acceleration; RF is on; $0 < t < t_{beam}$, $t=0$ corresponds to the end of filling process
- $V(t) = Vexp(-t/\tau)$, cavity discharge; RF is off, no beam. $t=0$ corresponds to the end of acceleration

Estimate:
- Energy, delivered by the RF source <u>to the beam</u> during the pulse
- Total energy, delivered by the RF source during the pulse;
- Total energy dissipated in the cavity wall during the pulse;
- Energy, required for refrigeration;
- Beam power /cavity (20 Hz repetition rate);
- Average RF power/cavity;
- Power necessary for refrigeration/cavity;
- Acceleration efficiency, the beam power over the sum of the RF power and power required for refrigeration.


‡ Fermilab

Homework

The ideal HWR cavity for β = 0.112 operates at frequency f = 162.5 MHz. It provides the energy gain (acceleration voltage) V = 2 MeV. The inner radius is a, the outer radius is b.

Estimate:

- The cavity length L;
- Effective cavity length;
- Acceleration gradient
- The optimal ratio b/a to achieve minimal surface electric field (on the inner electrode) at fixed b, taking into account that in a coaxial line $E_r \sim 1/r$;
- b and a to get maximal energy gain;
- The voltage difference U between the inner and outer electrodes at z=0.
- The coaxial impedance Z_c.
- The energy stored in the cavity;
- R/Q;
- The Ohmic loss in the cavity taking R_s=3 nOhm.
- Unloaded quality factor Q_0 and G-factor
- Maximal surface electric and magnetic fields and field enhancement factors K_B and K_E.

Si(x) calculator: https://keisan.casio.com/exec/system/1180573420
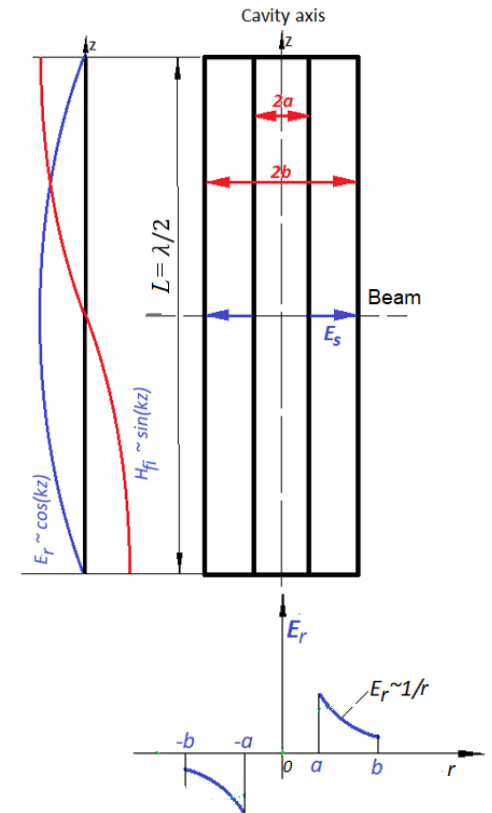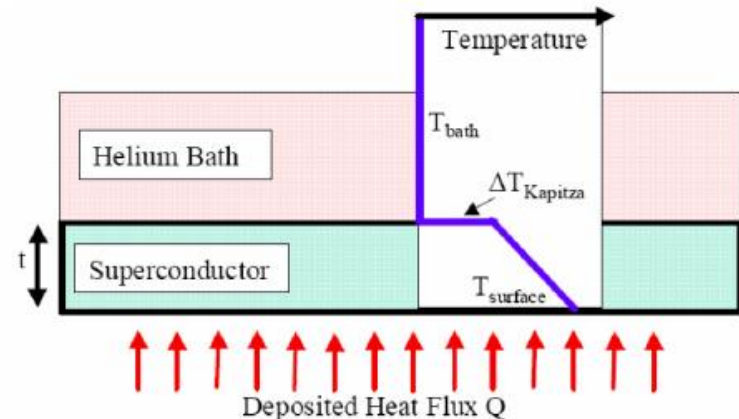
Homework

Task 4 (bonus problem)

Calculate the maximum temperature rise δT and maximum surface magnetic field H_b in the cavity, when cavity has thermal breakdown. For estimations take the following parameters:

- *Operating frequency:*   *f=3.9 GHz*
- *Helium temperature:* T_0=2°K
- *Niobium thickness:*   *d=3 mm*
- *Thermal conductivity*:* $k(T_0)$=30 W/(m•K)
- *Kapitsa resistance*:* $h(T_0)$=10⁴ W/(m²•K)
- *BCS surface resistance for Nb :*

$$R_s(T) = R_0 \cdot \left[\frac{f(GHz)}{1.3} \right]^2 \cdot \left(\frac{T_c}{T} \right) \cdot e^{-\Delta \cdot \frac{T_c}{T}} \quad , \ T \ll T_c$$

where: R_0=10⁻⁵ [Ω]; Δ=1.8 ; T_c=9.2°K
Use assumption, that temperature rise δT is small compared to T_0. Therefore, neglect temperature dependence of *k* and *h* (but not R_s!).

🔷 **Fermilab**

Appendixes

Fermilab

Appendix 1, Vector calculus

$\nabla \cdot (\psi \mathbf{A}) = \mathbf{A} \cdot \nabla \psi + \psi \nabla \cdot \mathbf{A}$	$\mathbf{div}(\psi \mathbf{A}) = \mathbf{A} \cdot \mathbf{grad}\psi + \psi\,\mathbf{div}\mathbf{A}$	
$\nabla \times (\psi \mathbf{A}) = \nabla \psi \times \mathbf{A} + \psi \nabla \times \mathbf{A}$	$\mathbf{rot}(\psi \mathbf{A}) = \mathbf{grad}\psi \times \mathbf{A} + \psi\,\mathbf{rot}\mathbf{A}$	
$\nabla(\mathbf{A} \cdot \mathbf{B}) = (\mathbf{A} \cdot \nabla)\mathbf{B} + (\mathbf{B} \cdot \nabla)\mathbf{A} +$ $+\mathbf{A} \times (\nabla \times \mathbf{B}) + \mathbf{B} \times (\nabla \times \mathbf{A})$	$\mathbf{grad}(\mathbf{A} \cdot \mathbf{B}) = (\mathbf{A} \cdot \nabla)\mathbf{B} + (\mathbf{B} \cdot \nabla)\mathbf{A} +$ $+\mathbf{A} \times \mathbf{rot}\mathbf{B} + \mathbf{B} \times \mathbf{rot}\mathbf{A}$	P.W.
$\frac{1}{2}\nabla A^2 = \mathbf{A} \times (\nabla \times \mathbf{A}) + (\mathbf{A} \cdot \nabla)\mathbf{A}$	$\frac{1}{2}\,\mathbf{grad}A^2 = \mathbf{A} \times (\mathbf{rot}\mathbf{A}) + (\mathbf{A} \cdot \nabla)\mathbf{A}$	
$\nabla \cdot (\mathbf{A} \times \mathbf{B}) = \mathbf{B} \cdot \nabla \times \mathbf{A} - \mathbf{A} \cdot \nabla \times \mathbf{B}$	$\mathbf{div}\,(\mathbf{A} \times \mathbf{B}) = \mathbf{B} \cdot \mathbf{rot}\,\mathbf{A} - \mathbf{A} \cdot \mathbf{rot}\,\mathbf{B}$	*
$\nabla \times (\mathbf{A} \times \mathbf{B}) = \mathbf{A}(\nabla \cdot \mathbf{B}) - \mathbf{B}(\nabla \cdot \mathbf{A}) +$ $+(\mathbf{B} \cdot \nabla)\mathbf{A} - (\mathbf{A} \cdot \nabla)\mathbf{B}$	$\mathbf{rot}(\mathbf{A} \times \mathbf{B}) = \mathbf{A}\,(\mathbf{div}\,\mathbf{B}) - \mathbf{B}\,(\mathbf{div}\,\mathbf{A}) +$ $+(\mathbf{B} \cdot \nabla)\mathbf{A} - (\mathbf{A} \cdot \nabla)\mathbf{B}$	

Fermilab

Appendix 1. Vector calculus

$\nabla \psi = \text{grad } \psi$

$\nabla \cdot \mathbf{A} = \text{div } \mathbf{A}$

$\nabla \times \mathbf{A} = \text{rot } \mathbf{A} \equiv \text{curl } \mathbf{A}$

$\Delta = \nabla^2 = \nabla \cdot \nabla$

$\nabla \times (\nabla \psi) = 0$	$\mathbf{rot}(\mathbf{grad} \ \psi) = 0$
$\nabla \cdot (\nabla \times \mathbf{A}) = 0$	$\mathbf{div} \ (\mathbf{rot \ A}) = 0$
$\Delta \psi = \nabla \cdot (\nabla \psi) = \nabla^2 \psi$	$\Delta \psi = \mathbf{div} \ (\mathbf{grad} \ \psi)$
$\nabla \times \nabla \times \mathbf{A} = \nabla(\nabla \cdot \mathbf{A}) - \nabla^2 \mathbf{A}$	$\mathbf{rot} \ (\mathbf{rot \ A}) = \mathbf{grad} \ (\mathbf{div \ A}) - \Delta \mathbf{A}$

$\nabla = \dfrac{\partial}{\partial x}\vec{i} + \dfrac{\partial}{\partial y}\vec{j} + \dfrac{\partial}{\partial z}\vec{k},$

$\displaystyle\int \text{rot } \mathbf{F} \cdot d\vec{S} = \oint \mathbf{F} \cdot d\boldsymbol{l} \ , \qquad \int \text{div } \mathbf{F} \ dV = \int \mathbf{F} \cdot d\vec{S}$

Stokes theorem   Gauss theorem

**Fermilab**

Appendix 1. Vector calculus

Differential operators in different coordinates:

	Cartesian	Cylindrical	Spherical
$\mathbf{A}$	$A_x\hat{\mathbf{x}} + A_y\hat{\mathbf{y}} + A_z\hat{\mathbf{z}}$	$A_\rho\hat{\boldsymbol{\rho}} + A_\varphi\hat{\boldsymbol{\varphi}} + A_z\hat{\mathbf{z}}$	$A_r\hat{\boldsymbol{r}} + A_\theta\hat{\boldsymbol{\theta}} + A_\varphi\hat{\boldsymbol{\varphi}}$
∇f	$\dfrac{\partial f}{\partial x}\hat{\mathbf{x}} + \dfrac{\partial f}{\partial y}\hat{\mathbf{y}} + \dfrac{\partial f}{\partial z}\hat{\mathbf{z}}$	$\dfrac{\partial f}{\partial \rho}\hat{\boldsymbol{\rho}} + \dfrac{1}{\rho}\dfrac{\partial f}{\partial \varphi}\hat{\boldsymbol{\varphi}} + \dfrac{\partial f}{\partial z}\hat{\mathbf{z}}$	$\dfrac{\partial f}{\partial r}\hat{\boldsymbol{r}} + \dfrac{1}{r}\dfrac{\partial f}{\partial \theta}\hat{\boldsymbol{\theta}} + \dfrac{1}{r\sin\theta}\dfrac{\partial f}{\partial \varphi}\hat{\boldsymbol{\varphi}}$
$\nabla \cdot \mathbf{A}$	$\dfrac{\partial A_x}{\partial x} + \dfrac{\partial A_y}{\partial y} + \dfrac{\partial A_z}{\partial z}$	$\dfrac{1}{\rho}\dfrac{\partial(\rho A_\rho)}{\partial \rho} + \dfrac{1}{\rho}\dfrac{\partial A_\varphi}{\partial \varphi} + \dfrac{\partial A_z}{\partial z}$	$\dfrac{1}{r^2}\dfrac{\partial(r^2 A_r)}{\partial r} + \dfrac{1}{r\sin\theta}\dfrac{\partial}{\partial \theta}(A_\theta\sin\theta) + \dfrac{1}{r\sin\theta}\dfrac{\partial A_\varphi}{\partial \varphi}$
$\nabla \times \mathbf{A}$	$\left(\dfrac{\partial A_z}{\partial y} - \dfrac{\partial A_y}{\partial z}\right)\hat{\mathbf{x}}\ +$ $\left(\dfrac{\partial A_x}{\partial z} - \dfrac{\partial A_z}{\partial x}\right)\hat{\mathbf{y}}\ +$ $\left(\dfrac{\partial A_y}{\partial x} - \dfrac{\partial A_x}{\partial y}\right)\hat{\mathbf{z}}$	$\left(\dfrac{1}{\rho}\dfrac{\partial A_z}{\partial \varphi} - \dfrac{\partial A_\varphi}{\partial z}\right)\hat{\boldsymbol{\rho}}\ +$ $\left(\dfrac{\partial A_\rho}{\partial z} - \dfrac{\partial A_z}{\partial \rho}\right)\hat{\boldsymbol{\varphi}}\ +$ $\dfrac{1}{\rho}\left(\dfrac{\partial(\rho A_\varphi)}{\partial \rho} - \dfrac{\partial A_\rho}{\partial \varphi}\right)\hat{\mathbf{z}}$	$\dfrac{1}{r\sin\theta}\left(\dfrac{\partial}{\partial \theta}(A_\varphi\sin\theta) - \dfrac{\partial A_\theta}{\partial \varphi}\right)\hat{\boldsymbol{r}}\ +$ $\dfrac{1}{r}\left(\dfrac{1}{\sin\theta}\dfrac{\partial A_r}{\partial \varphi} - \dfrac{\partial}{\partial r}(r A_\varphi)\right)\hat{\boldsymbol{\theta}}\ +$ $\dfrac{1}{r}\left(\dfrac{\partial}{\partial r}(r A_\theta) - \dfrac{\partial A_r}{\partial \theta}\right)\hat{\boldsymbol{\varphi}}$
$\Delta f = \nabla^2 f$	$\dfrac{\partial^2 f}{\partial x^2} + \dfrac{\partial^2 f}{\partial y^2} + \dfrac{\partial^2 f}{\partial z^2}$	$\dfrac{1}{\rho}\dfrac{\partial}{\partial \rho}\left(\rho\dfrac{\partial f}{\partial \rho}\right) + \dfrac{1}{\rho^2}\dfrac{\partial^2 f}{\partial \varphi^2} + \dfrac{\partial^2 f}{\partial z^2}$	$\dfrac{1}{r^2}\dfrac{\partial}{\partial r}\left(r^2\dfrac{\partial f}{\partial r}\right) + \dfrac{1}{r^2\sin\theta}\dfrac{\partial}{\partial \theta}\left(\sin\theta\dfrac{\partial f}{\partial \theta}\right) + \dfrac{1}{r^2\sin^2\theta}\dfrac{\partial^2 f}{\partial \varphi^2}$
$\Delta\mathbf{A}$	$\Delta A_x\hat{\mathbf{x}} + \Delta A_y\hat{\mathbf{y}} + \Delta A_z\hat{\mathbf{z}}$	$\left(\Delta A_\rho - \dfrac{A_\rho}{\rho^2} - \dfrac{2}{\rho^2}\dfrac{\partial A_\varphi}{\partial \varphi}\right)\hat{\boldsymbol{\rho}}\ +$ $\left(\Delta A_\varphi - \dfrac{A_\varphi}{\rho^2} + \dfrac{2}{\rho^2}\dfrac{\partial A_\rho}{\partial \varphi}\right)\hat{\boldsymbol{\varphi}}\ +$ $(\Delta A_z)\hat{\boldsymbol{z}}$	$\left(\Delta A_r - \dfrac{2A_r}{r^2} - \dfrac{2}{r^2\sin\theta}\dfrac{\partial(A_\theta\sin\theta)}{\partial \theta} - \dfrac{2}{r^2\sin\theta}\dfrac{\partial A_\varphi}{\partial \varphi}\right)\hat{\boldsymbol{r}}\ +$ $\left(\Delta A_\theta - \dfrac{A_\theta}{r^2\sin^2\theta} + \dfrac{2}{r^2}\dfrac{\partial A_r}{\partial \theta} - \dfrac{2\cos\theta}{r^2\sin^2\theta}\dfrac{\partial A_\varphi}{\partial \varphi}\right)\hat{\boldsymbol{\theta}}\ +$ $\left(\Delta A_\varphi - \dfrac{A_\varphi}{r^2\sin^2\theta} + \dfrac{2}{r^2\sin\theta}\dfrac{\partial A_r}{\partial \varphi} + \dfrac{2\cos\theta}{r^2\sin^2\theta}\dfrac{\partial A_\theta}{\partial \varphi}\right)\hat{\boldsymbol{\varphi}}$

Fermilab

Appendix 2, Panofsky-Wenzel theorem

Let's consider the particle transverse momentum change causes by the cavity RF field. The particle moves on the trajectory $z=vt$ parallel to the axis, but is displaced from it by $\vec{r}_\perp$.

Force acting on the particle is

$$\vec{F}(\vec{r}) = e\left[\vec{E}(\vec{r}) + \vec{v} \times \vec{B}(\vec{r})\right]e^{i\omega t}.$$

From Maxwell equation $rot\vec{E}(\vec{r}) = -i\omega\vec{B}(\vec{r})$ one has:

$$\vec{F}(\vec{r}) = e\left[\vec{E}(\vec{r}) + \vec{v} \times \frac{i}{\omega}rot\vec{E}(\vec{r})\right]e^{i\omega t} = e\left[\vec{E}(\vec{r}) + \frac{i}{\omega}\vec{\nabla}(\vec{v}\cdot\vec{E}(\vec{r})) - (\vec{v}\cdot\vec{\nabla})\cdot\vec{E}(\vec{r})\right]e^{i\omega t}.$$

If $\vec{v} = \vec{i}_z v$, then

$$F_z(\vec{r}) = eE_z(\vec{r})e^{i\omega t}$$

$$F_\perp(\vec{r}) = e\left[\vec{E}_\perp(\vec{r}) + v\frac{i}{\omega}\left(\vec{\nabla}_\perp E_z(\vec{r}) - \frac{\partial\vec{E}_\perp(\vec{r})}{\partial z}\right)\right]e^{i\omega t}$$

The differential operator $\vec{\nabla}_\perp$ acts on the transverse coordinates $\vec{r}_\perp$ only.

🔅 **Fermilab**

Appendix 2

If the particle velocity and particle transverse coordinates do not change significantly in the cavity, longitudinal and transverse momentum changes are:

$$\Delta p_{\|} = e\int_{-\infty}^{\infty} E_z(\vec{r})e^{i\omega t}dt\,|_{t=z/v} = \frac{e}{v}\int_{-\infty}^{\infty} E_z(\vec{r})e^{i\omega z/v}dz;$$

$$\Delta\vec{p}_{\perp} = e\int_{-\infty}^{\infty}\left[\vec{E}_{\perp}(\vec{r}) + \frac{iv}{\omega}\vec{\nabla}_{\perp}E_z(\vec{r}) - \frac{iv}{\omega}\frac{\partial\vec{E}_{\perp}(\vec{r})}{\partial z}\right]e^{i\omega t}dt\,|_{t=z/v}$$

However,

$$\frac{iv}{\omega}\int_{-\infty}^{\infty}\frac{\partial\vec{E}_{\perp}(\vec{r})}{\partial z}e^{i\omega t}dt\,|_{t=z/v} = \frac{i}{\omega}\int_{-\infty}^{\infty}\frac{\partial\vec{E}_{\perp}(\vec{r})}{\partial z}e^{i\omega z/v}dz = \frac{1}{v}\int_{-\infty}^{\infty}\vec{E}_{\perp}(\vec{r})e^{i\omega z/v}dz = \int_{-\infty}^{\infty}\vec{E}_{\perp}(\vec{r})e^{i\omega t}dt\,|_{t=z/v}$$

and

$$\Delta\vec{p}_{\perp} = e\frac{iv}{\omega}\int_{-\infty}^{\infty}\vec{\nabla}_{\perp}E_z(\vec{r})e^{i\omega t}dt\,|_{t=z/v} = e\frac{i}{\omega}\int_{-\infty}^{\infty}\vec{\nabla}_{\perp}E_z(\vec{r})e^{i\omega z/v}dz$$

Finally, we have:

$$\Delta\vec{p}_{\perp} = \frac{iv}{\omega}\vec{\nabla}_{\perp}(\Delta p_{\|}).$$

This relation between transverse and longitudinal momentum changes in an RF field is known as Panofsky – Wenzel theorem.

🍩 Fermilab

Appendix 3. Eigen modes properties:

Eigenmodes in a cavity.

$$\text{rot}\,\vec{E} = -i\omega\mu_0\vec{H}, \quad \text{rot}\,\vec{H} = i\omega\varepsilon_0\vec{E}$$

$$\text{rot}\,\text{rot}\,\vec{E} - k^2\vec{E} = 0, \quad \text{rot}\,\text{rot}\,\vec{H} - k^2\vec{H} = 0. \qquad (1)$$

Here $k^2 = \omega^2\varepsilon_0\mu_0$

Boundary conditions: $\vec{E}_t = 0, \; H_n = 0$ or $\vec{n}\times\vec{E} = 0, \vec{n}\cdot\vec{H} = 0$

Equations (1) has non-trivial solutions only for defined k_m^2 eigenvalues.

Corresponding solutions $\vec{E}_m(x,y,z)$ and $\vec{H}_m(x,y,z)$-eigenfunctions.

There are infinite number of eigenvalues.

Eigenvalues are **real** and **positive.** From (1) and vector theorem (App.1)

$$\text{div}(\vec{A}\times\vec{B}) = \vec{B}\cdot\text{rot}\vec{A} - \vec{A}\cdot\text{rot}\vec{B} \quad (2) \text{ one has:}$$

$$\text{div}\,(\vec{H}_m^*\times\text{rot}\,\vec{H}_m) = \text{rot}\,\vec{H}_m\cdot\text{rot}\,\vec{H}_m^* - \vec{H}_m^*\cdot\text{rot}\,\text{rot}\,\vec{H}_m = |\text{rot}\,\vec{H}_m|^2 - k_m^2\cdot|\vec{H}_m|^2.$$

0

$$k_m^2\int_V |\vec{H}_m|^2\,dV = \int_V |\text{rot}\,\vec{H}_m|^2\,dV - \oint_S (\vec{H}_m^*\times\text{rot}\,\vec{H}_m)\vec{n}\,dS. \qquad k_m^2 = \frac{\int_V |\text{rot}\,\vec{H}_m|^2\,dV}{\int_V |\vec{H}_m|^2\,dV}.$$

Fermilab

Appendix 3. Eigen modes properties

Eigenmodes are orthogonal:

$$\operatorname{rot}\operatorname{rot}\vec{E}_m \; - \; k_m^2\vec{E}_m \; = \; 0, \qquad k_m^2 \neq k_n^2 \qquad (3)$$
$$\operatorname{rot}\operatorname{rot}\vec{E}_n \; - \; k_n^2\vec{E}_n \; = \; 0.$$

Let's calculate using (2)

$$\operatorname{div}(\vec{E}_n \times \operatorname{rot}\vec{E}_m) \; - \; \operatorname{div}(\vec{E}_m \times \operatorname{rot}\vec{E}_n) \; = \; \operatorname{rot}\vec{E}_m \cdot \operatorname{rot}\vec{E}_n \; - \; \vec{E}_n \cdot \operatorname{rot}\operatorname{rot}\vec{E}_m \; -$$
$$- \; \operatorname{rot}\vec{E}_n \cdot \operatorname{rot}\vec{E}_m \; + \; \vec{E}_m \cdot \operatorname{rot}\operatorname{rot}\vec{E}_n \; = \; \vec{E}_m \cdot \operatorname{rot}\operatorname{rot}\vec{E}_n \; - \; \vec{E}_n \cdot \operatorname{rot}\operatorname{rot}\vec{E}_m.$$

Using (3) we have:

$$\operatorname{div}(\vec{E}_n \times \operatorname{rot}\vec{E}_m) \; - \; \operatorname{div}(\vec{E}_m \times \operatorname{rot}\vec{E}_n) \; = \; (k_n^2 \; - \; k_m^2)\vec{E}_m \cdot \vec{E}_n.$$

$$(k_n^2 \; - \; k_m^2)\int_V \vec{E}_m \cdot \vec{E}_n \, dV \; = \; \oint_S(\vec{E}_n \times \operatorname{rot}\vec{E}_m - \vec{E}_m \times \operatorname{rot}\vec{E}_n)\vec{n} \, dS.$$

0

$$(k_n^2 \; - \; k_m^2)\int_V \vec{E}_m \cdot \vec{E}_n \, dV \; = \; 0, \qquad k_m^2 \neq k_n^2$$

$$\boxed{\int_V \vec{E}_m \cdot \vec{E}_n \, dV \; = \; 0.}$$ and the same $$\boxed{\int_V \vec{H}_m \cdot \vec{H}_n \, dV \; = \; 0.}$$

🔷 **Fermilab**

Appendix 3. Eigen modes properties

Let's consider again the equation we got

$$k_m^2 \int_V |\vec{H}_m|^2 \, dV = \int_V |\text{rot}\,\vec{H}_m|^2 \, dV$$

Taking into account $\text{rot}\,\vec{H}_m = i\omega_m \varepsilon_0 \vec{E}_m$ and $k_m^2 = \omega_m^2 \cdot \mu_0 \varepsilon_0$, we have:

$$\int_V \frac{\mu_0 |H_m|^2}{4} \, dV = \int_V \frac{\varepsilon_0 |E_m|^2}{4} \, dV,$$

The time-average electrical stored energy is equal to the time-average magnetic stored energy.

🎇 **Fermilab**

Appendix 3. Eigen modes properties:

Variation properties of the eigenmodes:

$$k^2 = \frac{\int |\mathrm{rot}\, H|^2\, dV}{\int |H|^2\, dV},$$

$$\mathrm{rot}\,\mathrm{rot}\,\vec{H} - k^2\vec{H} = 0$$

boundary conditions: $\vec{n} \times \mathrm{rot}\,\vec{H} = 0$

Variation gives:

$$\delta k^2 \int_V |\vec{H}|^2\, dV = 2\int_V (\mathrm{rot}\,\mathrm{rot}\,\vec{H} - k^2\vec{H})\cdot\delta\vec{H}\, dV + \int_V \mathrm{div}\,(\delta\vec{H} \times \mathrm{rot}\,\vec{H})\, dV.$$

$$\delta k^2 \int_V |H|^2\, dV + 2k^2\int_V \vec{H}\,\delta\vec{H}\, dV = 2\int_V \mathrm{rot}\,\vec{H}\,\mathrm{rot}\,\delta\vec{H}\, dV.$$

The vector theorem has been used:

$$\mathrm{div}\,(\delta\vec{H} \times \mathrm{rot}\,\vec{H}) = \mathrm{rot}\,\vec{H}\cdot\mathrm{rot}\,\delta\vec{H} - \delta\vec{H}\cdot\mathrm{rot}\,\mathrm{rot}\,\vec{H},$$
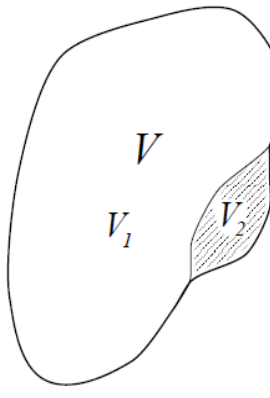
Using Gauss theorem on has:

$$\delta k^2 \int_V |\vec{H}|^2\, dV = 2\int_V (\mathrm{rot}\,\mathrm{rot}\,\vec{H} - k^2\vec{H})\cdot\delta\vec{H}\, dV - \oint_S (\vec{n} \times \mathrm{rot}\,\vec{H})\cdot\delta\vec{H}\, dS = 0$$

$$\boxed{\delta k^2 = 0}$$

🔷 Fermilab

Appendix 3.

Small perturbations of the cavity geometry:

$$k^2 = \frac{\int\limits_{V_1} |\mathrm{rot}\,\vec{H}^{(2)}|^2\, dV}{\int\limits_{V_1} |\vec{H}^{(2)}|^2\, dV} \approx \frac{\int\limits_{V_1} |\mathrm{rot}\,\vec{H}^{(1)}|^2\, dV}{\int\limits_{V_1} |\vec{H}^{(1)}|^2\, dV} = \frac{\int\limits_{V} |\mathrm{rot}\,\vec{H}^{(1)}|^2\, dV - \int\limits_{V_2} |\mathrm{rot}\,\vec{H}^{(1)}|^2\, dV}{\int\limits_{V} |\vec{H}^{(1)}|^2\, dV - \int\limits_{V_2} |\vec{H}^{(1)}|^2\, dV} =$$

$$= k_1^2 \left\{ 1 + \frac{\int\limits_{V_2} |\vec{H}^{(1)}|^2\, dV}{\int\limits_{V} |\vec{H}^{(1)}|^2\, dV} - \frac{\int\limits_{V_2} |\mathrm{rot}\,\vec{H}^{(1)}|^2\, dV}{\int\limits_{V} |\mathrm{rot}\,\vec{H}^{(1)}|^2\, dV} \right\} = k_1^2 \left(1 + \frac{\Delta W_E - \Delta W_H}{W_0} \right)$$

$$\frac{k^2 - k_1^2}{k_1^2} = \frac{\Delta W_E - \Delta W_H}{W_0} \approx \frac{2\Delta\omega}{\omega_1} = \frac{(w_E - w_H)\cdot\Delta V}{W_0}. \quad \leftarrow\text{Slater theorem}$$

On the other hand, $\quad \frac{1}{2}(w_H - w_E)\Delta V = p\,\Delta V = -\Delta W_0 \quad$ and

$$\frac{\Delta\omega}{\omega_0} = \frac{\Delta W_0}{W_0},$$

$$\boxed{\frac{W_0}{\omega_0} = \mathrm{const}} \quad \text{(compare to } E{=}vh\text{)}$$

🎇 **Fermilab**

Appendix 4: Accelerating voltage and transit time factor:

For arbitrary axial distribution of the axisymmetric accelerating filed the voltage $V(\varphi)$ at arbitrary phase φ is the following:

$$V(\varphi) = Re \int_{-\infty}^{\infty} E_z(\rho = 0, z) e^{i(k_z z + \varphi)} dz =$$

$$= \int_{-\infty}^{\infty} Re[E_z(\rho = 0, z)] \cos(k_z z + \varphi) dz - \int_{-\infty}^{\infty} Im[E_z(\rho = 0, z)] \sin(k_z z + \varphi) dz =$$

$$= \int_{-\infty}^{\infty} Re[E_z(\rho = 0, z)] \cos(k_z z + \varphi) dz - \int_{-\infty}^{\infty} Im[E_z(\rho = 0, z)] \sin(k_z z + \varphi) dz =$$

$$= \cos(\varphi) \left(\int_{-\infty}^{\infty} Re[E_z(\rho = 0, z)] \cos(k_z z) dz - \int_{-\infty}^{\infty} Im[E_z(\rho = 0, z)] \sin(k_z z) dz \right) -$$

$$- \sin(\varphi) \left(\int_{-\infty}^{\infty} Re[E_z(\rho = 0, z)] \sin(k_z z) dz - \int_{-\infty}^{\infty} Im[E_z(\rho = 0, z)] \cos(k_z z) dz \right)$$

Maximal voltage *V* is, therefore,

$$V = \left[\left(\int_{-\infty}^{\infty} Re[E_z(\rho = 0, z)] \cos(k_z z) dz - \int_{-\infty}^{\infty} Im[E_z(\rho = 0, z)] \sin(k_z z) dz \right)^2 \right.$$

$$\left. + \left(\int_{-\infty}^{\infty} Re[E_z(\rho = 0, z)] \sin(k_z z) dz - \int_{-\infty}^{\infty} Im[E_z(\rho = 0, z)] \cos(k_z z) dz \right)^2 \right]^{1/2}$$

If $E_z(\rho, z)$ is real, $V = \left[\left(\int_{-\infty}^{\infty} E_z(\rho = 0, z) \cos(k_z z) dz \right)^2 + \left(\int_{-\infty}^{\infty} E_z(\rho = 0, z) \sin(k_z z) dz \right)^2 \right]^{1/2}$

🟠 **Fermilab**

Appendix 5. Modes in a pillbox cavity:

In a pillbox cavities resonance field satisfies wave equations:

$$\Delta \vec{E} + k^2 \vec{E} = 0, \Delta \vec{H} + k^2 \vec{H} = 0, \text{ where } k = \frac{\omega}{c} \text{ - wavenumber.}$$

For an ideally conductive wall components of electric field tangential to the surface is zero. The pillbox cavity may be considered as a part of a waveguide having circular cross section, shortened at both ends. The fields in this waveguide may be described in cylindrical coordinates, *(r,φ,z)*. In cylindrical coordinates longitudinal field components satisfy scalar wave equations:

$$\Delta E_z + k^2 E_z = 0, \Delta H_z + k^2 H_z = 0 \qquad\qquad (1)$$

For the waveguide, the fields have translation symmetry along $\vec{z}$, i.e., in two points having the same transverse coordinate, but different z, the fields differ by phase $\psi = k_z z$; *i.e.,* $\vec{E}, \vec{H} \sim e^{ik_z z}$. In this case:

- Equations (1) have solution

  $E_z(r, \varphi, z), H_z(r, \varphi, z) = J_m(k_r r) e^{im\varphi} e^{ik_z z}; J_m(k_r r)$ are Bessel functions;

- $k_r^2 + k_z^2 = k^2$;

- All transverse components (E_r, E_φ, H_r and H_φ)may be expressed through the longitudinal field components, E_z and H_z ;

- At *r=b* (*b* is the waveguide radius) E_z=0 and $\frac{\partial H_z}{\partial n} = 0.$ $\vec{n}$ is normal to the waveguide surface.

🟦 **Fermilab**
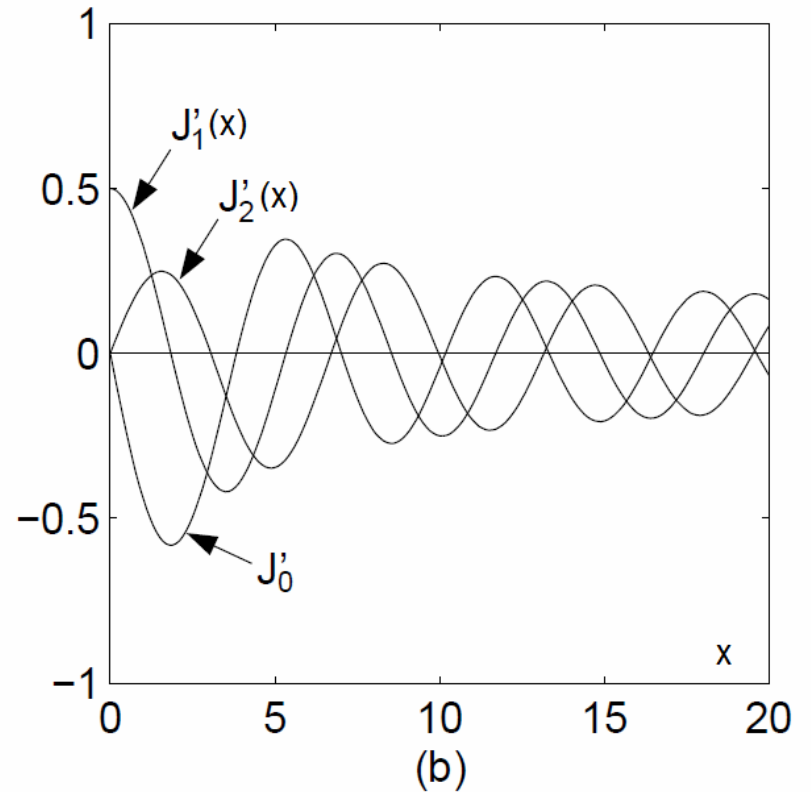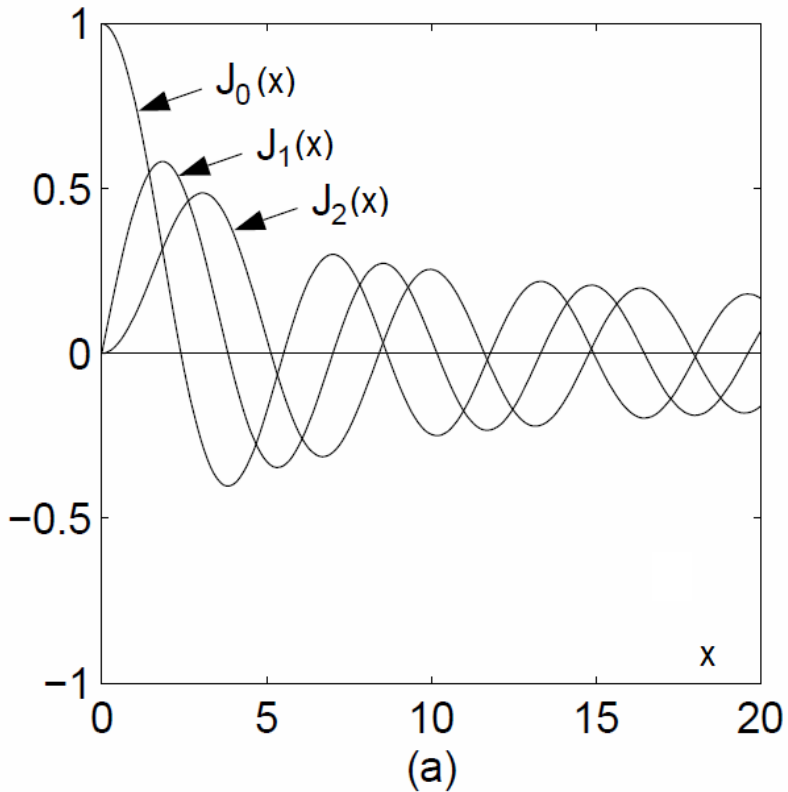
Appendix 5.

Bessel functions and their derivatives

🔀 **Fermilab**

Appendix 5.

E_z and H_z satisfy the same equation, but have different boundary conditions, and therefore, different k_r :

	Electric field:	**Magnetic field:**
Equation:	$\Delta E_z + k^2 E_z = 0$	$\Delta H_z + k^2 H_z = 0$
Boundary condition:	$E_z(r,\varphi,z) = 0, r = a;$	$\partial H_z(r,\varphi,z)/\partial r = 0, r = a$
or	$J_m(k_r b) = 0;$	$J'_m(k_r b) = 0,$
and	$k_r = \frac{\nu_{mn}}{b}; \ J_m(\nu_{mn}) = 0;$	$k_r = \frac{\mu_{mn}}{b}; \ J'_m(\mu_{mn}) = 0.$

For the pillbox cavity having end walls at z=0 and z=d; therefore $k_z d = \pi p$ and

$$E_z = CJ_m(k_r r)e^{im\varphi}\cos(\pi p z/d); \ H_z = J_m(k_r r)e^{im\varphi}\sin(\pi p z/d),$$

and resonant frequencies are:

$$\frac{\omega}{c} = \sqrt{\left(\frac{\nu_{mn}}{b}\right)^2 + \left(\frac{\pi p}{d}\right)^2} \ ; \qquad \frac{\omega}{c} = \sqrt{\left(\frac{\mu_{mn}}{b}\right)^2 + \left(\frac{\pi p}{d}\right)^2}$$

$$m = 0,1,..,\infty; \qquad\qquad m = 0,1,..,\infty;$$
$$n = 1,2,..,\infty; \qquad\qquad n = 1,2,..,\infty;$$
$$p = 0,1,..,\infty; \qquad\qquad p = 1,2,..,\infty;$$

<div style="color:red">TM_{mnp}-modes</div> <div style="color:blue">TE_{mnp}-modes</div>

$\textcolor{red}{\text{TM}_{mnp}\text{-modes}}$ $\textcolor{blue}{\text{TE}_{mnp}\text{-modes}}$

🎸 **Fermilab**

Appendix 5.

Roots of $J'_m(x) = 0$.

m	μ_{m1}	μ_{m2}	μ_{m3}	μ_{m4}
0	3.832	7.016	10.174	13.324
1	1.841	5.331	8.536	11.706
2	3.054	6.706	9.970	13.170
3	4.201	8.015	11.346	14.586
4	5.318	9.282	12.682	15.964
5	6.416	10.520	13.987	17.313

Roots of $J_m(x) = 0$.

m	ν_{m1}	ν_{m2}	ν_{m3}	ν_{m4}
0	2.405	5.520	8.654	11.792
1	3.832	7.016	10.174	13.324
2	5.135	8.417	11.620	14.796
3	6.380	9.761	13.015	16.223
4	7.588	11.065	14.373	17.616
5	8.771	12.339	15.700	18.980

$\mu_{0n} = \nu_{1n}$!

TM$_{1np}$ and TE$_{0np}$ are degenerated!
n=1,2,…, ∞;
p=1,2,…, ∞*

*Note that TE$_{0n0}$ does not exist because of boundary conditions for magnetic field on the end walls.

🟦 **Fermilab**

Appendix 5.

(1) TE_{11} (2) TM_{01} (3) TE_{21} (4) TM_{11} (5) TE_{01} (6) TE_{31}

(7) TM_{21} (8) TE_{41} (9) TE_{12} (10) TM_{02} (11) TM_{31} (12) TE_{51}

(13) TE_{22} (14) TE_{02} (15) TM_{12} (16) TE_{61} (17) TM_{41} (18) TE_{32}

(19) TM_{22} (20) TE_{13} (21) TE_{71} (22) TM_{03} (23) TM_{51} (24) TE_{42}

(25) TE_{81} (26) TM_{32} (27) TM_{61} (28) TE_{23} (29) TM_{13} (30) TE_{03}
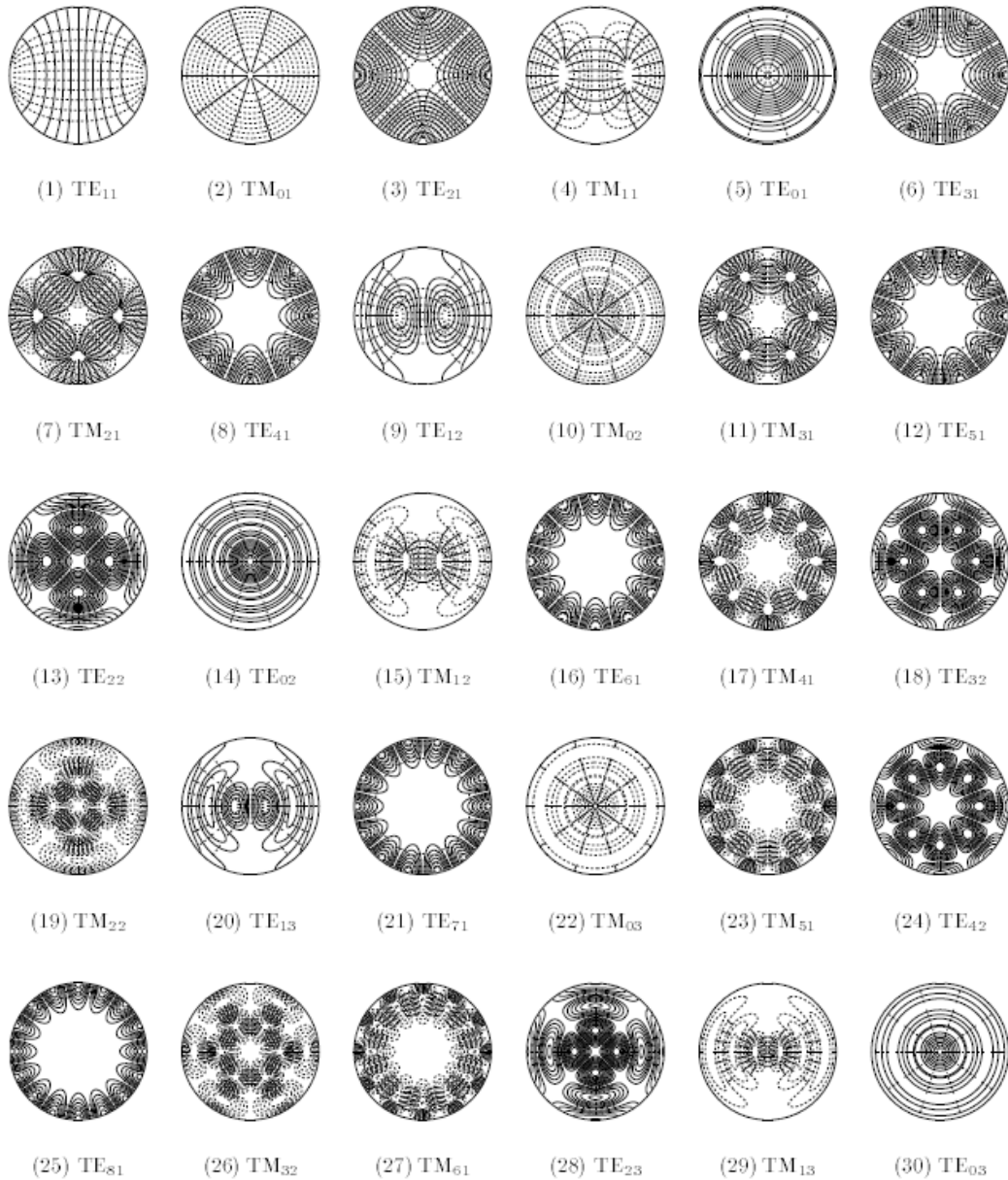
Field plots for the pillbox modes

‡ Fermilab

Appendix 6: RF cavity excitation by the beam:

- RF cavity having eigenmodes: eigen fields satisfy Maxwell equations:

$$\text{rot } \mathbf{E}_s = -i\omega_s\mu\mathbf{H}_s, \quad \text{rot } \mathbf{H}_s = i\omega_s\varepsilon\mathbf{E}_s. \tag{1}$$

- The field excited by the beam:

$$\text{rot } \mathbf{E} = -i\omega\mu\mathbf{H}, \tag{2}$$

$$\text{rot } \mathbf{H} = i\omega\varepsilon\mathbf{E} + \mathbf{J}_e$$

$\mathbf{J}_e$ – the beam current density spectrum component oscillating at the frequency ω

- The excited field may be expanded over the eigenmodes:

$$\mathbf{E} = \sum_s A_s\mathbf{E}_s - \text{grad }\varphi_e, \quad \mathbf{H} = \sum_s B_s\mathbf{H}_s \tag{3}$$

Here φ_e is space charge potential, typically its impact is small.

- From (1) and (2) one has:

$$\text{div}(\mathbf{E}_s^* \times \mathbf{H}) = \mathbf{H} \cdot (i\omega_s\mu\mathbf{H}_s^*) - \mathbf{E}_s^* \cdot (i\omega\varepsilon\mathbf{E} + \mathbf{J}_e) =$$
$$= i\omega_s\mu\mathbf{H} \cdot \mathbf{H}_s^* - i\omega\varepsilon\mathbf{E} \cdot \mathbf{E}_s^* - \mathbf{J}_e \cdot \mathbf{E}_s^*, \tag{4}$$
$$\text{div}(\mathbf{E} \times \mathbf{H}_s^*) = \mathbf{H}_s^* \cdot (-i\omega\mu\mathbf{H}) - \mathbf{E} \cdot (-i\omega_s\varepsilon\mathbf{E}_s^*) =$$
$$= -i\omega\mu\mathbf{H} \cdot \mathbf{H}_s + i\omega\varepsilon\mathbf{E} \cdot \mathbf{E}_s^*.$$

All the fields have zero tangential electric field components on the wall.

🔷 Fermilab

Appendix 6:

Substituting (3) to (4) one has:

$$A_s = -\frac{\omega}{i(\omega^2 - \omega_s^2)} \cdot \frac{\int_V \mathbf{J}_e \mathbf{E}_s^* \, dV}{\mu \int_V \mathbf{H}_s \cdot \mathbf{H}_s^* \, dV}, \qquad B_s = -\frac{\omega_s}{i(\omega^2 - \omega_s^2)} \cdot \frac{\int_V \mathbf{J}_e \mathbf{E}_s^* \, dV}{\mu \int_V \mathbf{H}_s \cdot \mathbf{H}_s^* \, dV},$$

Note that

$$\mu \int_V \mathbf{H}_s \cdot \mathbf{H}_s^* \, dV = 2W_s$$

If there are wall losses, $\qquad \omega_s^2 \rightarrow \omega_s^2\left(1 + \dfrac{i}{Q_0}\right)$

and for thin beam having the <u>average</u> current I_0 on the axis one has:

$$A_s = -\frac{i\omega}{\omega^2 - \omega_s^2 - i\frac{\omega\omega_s}{Q_s}} \times \frac{\int \mathbf{J}_e \mathbf{E}_s \, dV}{2W_s} = -\frac{i\omega}{\omega^2 - \omega_s^2 - i\frac{\omega\omega_s}{Q_s}} \times \frac{I_0 \left| \int_{-\infty}^{\infty} E_{sz}(z)e^{ikz} dz \right|}{W_s}, \quad k = \frac{\omega_s}{c} \qquad (5)$$

From (5) and (3) one has for the cavity voltage on the axis for the sth mode:

$$V_s = \frac{\Delta p_\parallel c}{e} = \int_{-\infty}^{\infty} E_{sz} e^{ikz} dz \approx \frac{i\omega_s^2}{\omega^2 - \omega_s^2 - i\frac{\omega\omega_s}{Q_s}} \cdot \frac{I_0 \left| \int_{-\infty}^{\infty} E_{sz}(z)e^{ikz} dz \right|^2}{\omega_s W_s} = \frac{i\omega_s^2}{\omega^2 - \omega_s^2 - i\frac{\omega\omega_s}{Q_s}} \cdot I_0 \left(\frac{R}{Q}\right)_s,$$

🟠 **Fermilab**

Appendix 6:

here

$$\left(\frac{R}{Q}\right)_s = \frac{\left|\int_{-\infty}^{\infty} E_{sz}(z)e^{ikz}dz\right|^2}{\omega_s W_s}$$

At the resonance one has

$$V_s = -Q_s I_0 \left(\frac{R}{Q}\right)_s = -I_0 R_s$$

where

$$R_s = Q_s \left(\frac{R}{Q}\right)_s$$

is a shunt impedance of the sth mode.

‎💠 Fermilab

Appendix 6:

- This coincides to the voltage excited by the AC current $I = -2I_0$ in a parallel resonance circuit.
- Note that for a short bunch the beam current spectrum is

$I(\omega) \approx I_0 + 2I_0 \sum \delta(\omega_s)$,

ω_s is the bunch sequence frequency; the equivalent circuit describes the cavity excitation by imaginary current, it gives the sign "-".

- From Kirchhoff theorem one has

$I_C + I_L + I_R = iV\omega C + V/R + V/i\omega L = -2I_0$,

and taking into account that $\omega_s = (LC)^{-1/2}$, we get

$$V_s = \frac{i\omega_s^2}{\omega^2 - \omega_s^2 - i\frac{\omega\omega_s}{Q_s}} \cdot I_0 \left(\frac{R}{Q}\right)_s,$$

if $\omega_s \approx \omega$. Here are the equivalent circuit parameters:

$L = (R/Q)_s/2\omega;$

$C = 2/\omega(R/Q)_s;$

$R = (R/Q)Q_s/2.$

🔶 **Fermilab**
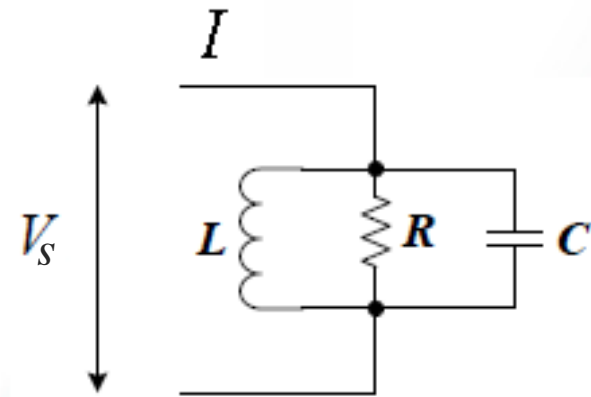
Appendix 7: The cavity coupled to the line.

Let's consider the cavity coupled to the feeding line:

Coupling slot

Cavity | line
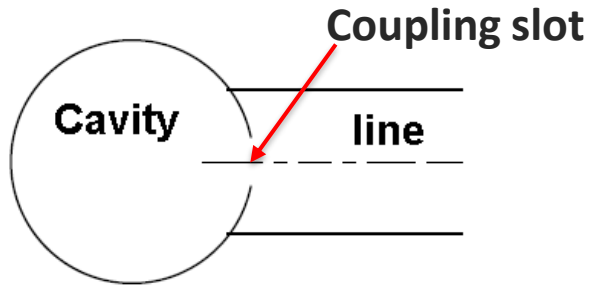
Consider another problem – the cavity coupled to the line shortened by a perfectly conducting plane S_1 placed such a way, that the electric field at the coupling slot has no tangential component:

Coupling slot S_1

Cavity | line   Cavity | line

(1)   (2) $E_t=0$
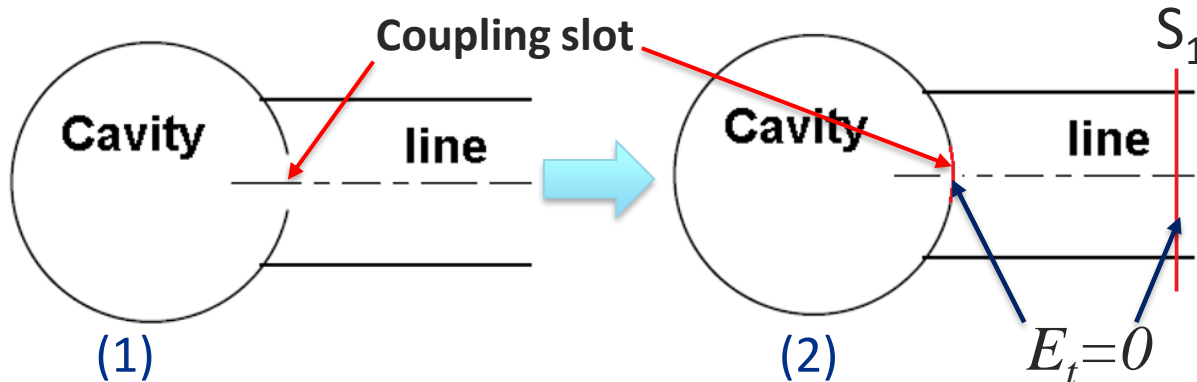
- The eigenfrequency of the new problem will be the same as for uncoupled cavity;
- The fields inside the cavity will be the same as for uncoupled cavity;
- The magnetic field on will be proportional to WG magnetic transverse eigenfunction h, $H_t=ik\boldsymbol{h}(x,y)$; k is coefficient (real for convenience). Tangential electric field is zero.

🎇 Fermilab

Appendix 7:

For the cavity excited by the line (problem 1) one has on S$_1$ for transverse fields:

$$E_t = U \cdot e(x,y), \ H_t = I \cdot h(x,y), \hspace{3cm} (1)$$

where $e(x,y)$ is the electric WG transverse eigenfunction, $\int_{S_1} (e \times h) dS = 1$.

The field in the cavity H is proportional to the eigenfunction H_s of the cavity coupled to the shortened line (see previous slide):

$$H = B \cdot H_s = ikBh(x,y) \hspace{3cm} (2)$$

From (1) and (2) one can find that

$$I = ikB \hspace{3cm} (3)$$

Following the procedure from Appendix 1 for the Lecture 2, we have, see Formulas 1,2 and 3 from this Appendix 1 and (1-3):

$$B = \frac{i\omega_s}{\omega^2 - \omega_s^2} \cdot \frac{\int_{S_I} \left(\vec{E} \times \vec{H}_s^*\right) \cdot dS}{2W_s} = -\frac{\omega_s}{\omega^2 - \omega_s^2} \cdot \frac{Uk}{2W_s}$$

and

$$\hspace{14cm} (4)$$

$$I = -\frac{i\omega_s}{\omega^2 - \omega_s^2} \cdot \frac{Uk^2}{2W_s}$$

Appendix 7:

If there is wall loss in the cavity, $\omega_s^2 \to \omega_s^2 \left(1 + \frac{i}{Q_0}\right)$ and

$$I = -\frac{i\omega_s}{\omega^2 - \omega_s^2 - \frac{i\omega_s^2}{Q_0}} \cdot \frac{Uk^2}{2W_s}.$$

The cavity impedance at S$_1$ is therefore

$$Z_1 = -R \left(\frac{\omega^2 - \omega_s^2 - \frac{i\omega_s^2}{Q_0}}{i\omega_s^2}\right) \approx R_1(1 + iQ_0 x), \qquad (5)$$
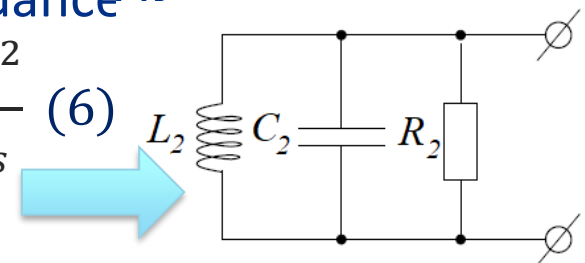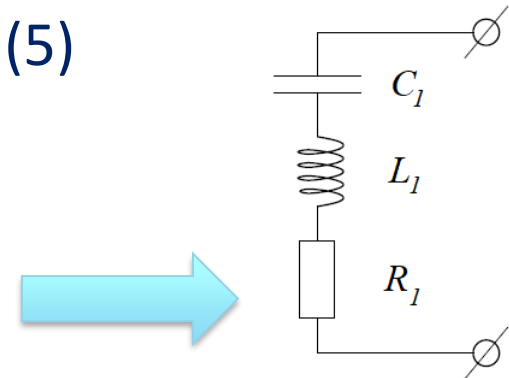
where

$$R_1 = \frac{2\omega_s W_s}{Q_0 k^2}, x = \frac{\omega^2}{\omega_s^2} - 1 \approx \frac{2(\omega - \omega_s)}{\omega_s}.$$

The impedance (5) coincides to the impedance of a serial resonance circuit . At the distance of $\Lambda/4$ (Λ is wavelength in the WG) the cavity impedance is
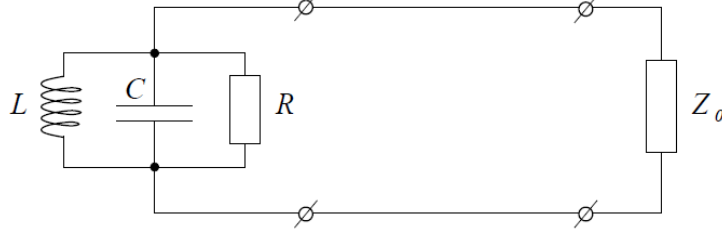
$$Z_2 = \frac{Z_0^2}{Z_1} = \frac{Z_0^2}{R_1(1 + iQ_0 x)} = \frac{R_2}{(1 + iQ_0 x)}, R_2 = \frac{Z_0^2 Q_0 k^2}{2\omega_s W_s} \quad (6)$$

It is the impedance of a parallel resonance circuit (Z_0 is the WG impedance).

Appendix 7:

If the line is matched, the equivalent circuit is

- Power P_R dissipated in R corresponds to the Ohmic losses in the cavity walls;
- Power P_{Z_0} dissipated in Z_0 corresponds to radiation in the line.

One can see:

$$\frac{P_{Z_0}}{P_R} = \frac{R}{Z_0} = \frac{Q_0}{Q_{ext}},$$

External quality factor, Q_{ext} describes radiation to the line:

$$Q_{ext} = \frac{\omega_s W_s}{P_{Z_0}}$$

Note that $Q_0 = \frac{\omega_s W_s}{P_R}$. The total loss is described by the loaded quality factor, Q_{load}

$$\frac{1}{Q_{load}} = \frac{P_{Z_0} + P_R}{\omega_s W_s} = \frac{1}{Q_{ext}} + \frac{1}{Q_0} \qquad (7)$$

Ratio of Q_0 to Q_{ext} is called coupling, β :

$$\frac{Q_0}{Q_{ext}} = \frac{R}{Z_0} \equiv \beta \qquad (8)$$

🔵 **Fermilab**

Appendix 7:

Let's estimate the reflection coefficient Γ of the parallel resonance circuit connected to the line:

$$\Gamma = \frac{Z - Z_0}{Z + Z_0},$$

According to (6)

$$Z = \frac{R}{(1 + iQ_0 x)}$$

At resonance ($x=0$)

$$\Gamma_0 = \frac{R - Z_0}{R + Z_0} = \frac{\frac{R}{Z_0} - 1}{\frac{R}{Z_0} + 1} = \frac{\beta - 1}{\beta + 1}.$$
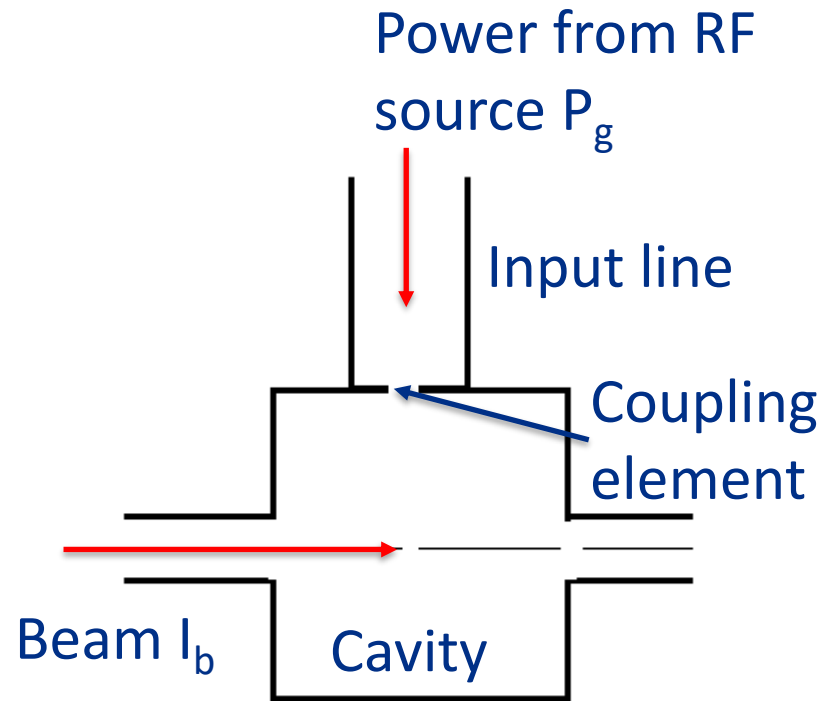
For $x{\neq}0$ one has

$$\Gamma = \frac{R - Z_0(1 + iQ_0 x)}{R + Z_0(1 + iQ_0 x)} = \frac{\Gamma_0 + 1}{1 + iQ_0 x/(1 + \beta)} - 1 = \frac{\Gamma_0 + 1}{1 + iQ_{load} x} - 1$$

(from (7) and (8) it follows that $Q_0/(1 + \beta) = Q_{load}$).

The power P dissipated in the cavity exited by the input power P_{in} is the following:

$$P = P_{in}(1 - |\Gamma|^2) = P_{in} \frac{1 - \Gamma_0^2}{1 + Q_{load}^2 x^2}.$$

🔷 **Fermilab**

Appendix 8: Beam Loading

Power from RF source P_g

Input line

Coupling element

Beam I_b

Cavity

- RF source and beam $\omega_g = \omega_b = \omega;$
- Cavity: ω_0
- Cavity voltage : V_c
- Shunt impedance: R_{sh}
- Losses: $P_c = V_c^2/R_{sh} = V_c^2/(Q_0 \cdot R/Q)$
- Radiation to the line: $V_c^2/(Q_{ext} \cdot R/Q)$
- Coupling: $\beta = Q_0/Q_{ext}$
- Loaded Q: $Q_L = Q_0/(1+\beta)$
- Average beam current: I_b
- Synchronous phase: φ
- Power consumed by the beam: $P_b = I_b V_c cos\varphi$
- Input power P_g
- Reflected power: $P_r = P_g - P_c - P_b$

🔷 **Fermilab**

Appendix 8:

Equivalent circuit for the cavity excited by a WG and loaded by the beam (transformed to the cavity):

WG   Cavity   Beam
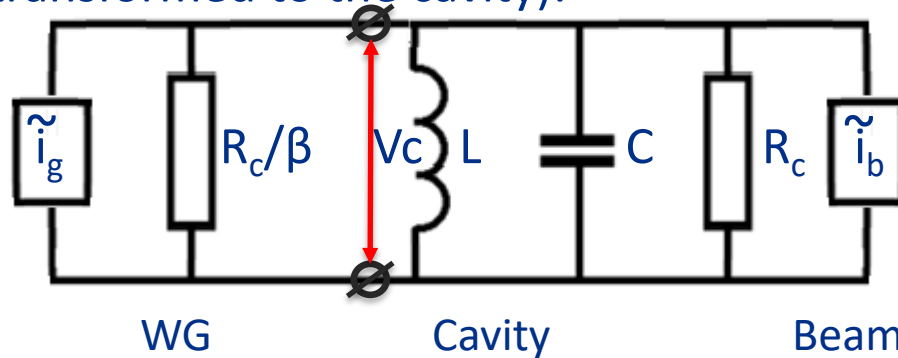
$$L = R/Q/(2\omega_0)$$
$$C = 2/(R/Q \cdot \omega_0)$$
$$R_c = R/Q \cdot Q_0/2$$
$$\tilde{\imath}_b = -2I_b$$
$$\beta = Q_0/Q_{ext}$$

- The WG impedance transformed to the cavity is $Z_{WG} = R_c/\beta$ (radiated power is $\frac{V_c^2}{R_c/\beta}$);

- The WG is terminated by the cavity impedance* $Z_0 = \frac{R_c}{1+iQ_0x}$ in parallel to the beam impedance $Z_b = \frac{V_c}{I_b e^{i\varphi}}$, φ is the beam phase versus the voltage V_c.

- The total load impedance is $Z = \left(\frac{1}{Z_0} + \frac{1}{Z_b}\right)^{-1} = \left(\frac{1+iQ_0x}{R_c} + \frac{I_b e^{i\varphi}}{V_c}\right)^{-1}$.

- Reflection for this load is $\Gamma = \frac{V_{ref}}{V_{forw}} = \frac{Z-Z_{WG}}{Z+Z_{WG}} = \frac{1 - Z_{WG}/Z}{1 + Z_{WG}/Z}$.

- The cavity voltage is $V_c = V_{ref} + V_{forw} = V_{forw}(1 + \Gamma) = V_{forw}\frac{2}{1 + Z_{WG}/Z}$ and

$V_{forw} = \frac{V_c}{(1+\Gamma)} = \frac{V_c}{2}\left(1 + Z_{WG}/Z\right)$.   *See Formulas (5-6), Appendix 7

≹ Fermilab

Appendix 8:

Therefore, the input power is:

$$P_g = \frac{|V_{forw}|^2}{Z_{WG}} = \frac{V_c^2}{4Z_{WG}}\left|1 + \frac{Z_{WG}}{Z}\right|^2 =$$

$$\approx \frac{V_c^2(1+\beta)^2}{4\left(\frac{R}{Q}\right)\beta Q_0}\left[\left(1 + \frac{I_b\cos\varphi\left(\frac{R}{Q}\right)Q_0}{(1+\beta)V_c}\right)^2 + \left(\frac{Q_0}{1+\beta}\cdot\frac{2\Delta f}{f} + \frac{I_b\sin\varphi\left(\frac{R}{Q}\right)Q_0}{1+\beta}\right)^2\right].$$

The formula works next to resonance: approximation is used for x:

$$x = \frac{\omega^2}{\omega_0^2} - 1 \approx \frac{2(\omega - \omega_0)}{\omega_0} = \frac{2(f - f_0)}{f_0} \approx \frac{2(f - f_0)}{f} = \frac{2\Delta f}{f}.$$

Note that $P_g = \frac{|V_{forw}|^2}{Z_{WG}}$ does not contain factor of 2 in the denominator

because of the cavity impedance $\left(\frac{R}{Q}\right)$ definition.

🎇 **Fermilab**

Appendix 9: Transverse impedance:

Let's consider a cavity excited by a beam current I_0 having offset x_0. If $\vec{E}$ is a dipole eigenmode, the field $\vec{\mathbf{E}}$ in the cavity in one-mode approximation may be expressed as $\vec{\mathbf{E}} \approx A(\omega, \omega_0)\vec{E}$, where ω is the bunch sequence harmonic frequency, ω_0 is the resonant frequency, and

$$A = -\frac{i\omega}{\omega^2 - \omega_0^2 - i\frac{\omega\omega_0}{Q}} \times \frac{\int \vec{j} \cdot \vec{\mathbf{E}}dV}{2W} = -\frac{i\omega}{\omega^2 - \omega_0^2 - i\frac{\omega\omega_0}{Q}} \times \frac{I_0\left|\int_{-\infty}^{\infty} E_z(x,y,z)e^{ikz}dz\right|}{W}.$$

where $\quad W = \frac{\varepsilon_0}{2}\int |\vec{E}|^2 dV \quad$ and I_0 is <u>an average </u>current

₹ Fermilab

Appendix 10:

RF-kick at $x = x_0$ and $y=0$ may be obtained using Panofsky-Wenzel theorem:

$$U_{kick} = \frac{\Delta p_\perp c}{e} = \frac{ic}{\omega}\left|\nabla_\perp \int_{-\infty}^{\infty} E_z\, e^{ikz}\, dz\right| \approx \frac{c}{x_0\left(\omega^2 - \omega_0^2 - i\frac{\omega\omega_0}{Q}\right)} \times \frac{I_0\left|\int_{-\infty}^{\infty} E_z(x_0,0,z)e^{ikz}dz\right|^2}{W}$$

$$\approx \frac{c\omega_0}{\left(\omega^2 - \omega_0^2 - i\frac{\omega\omega_0}{Q}\right)} \times \frac{x_0 I_0\left|\int_{-\infty}^{\infty}\left(\frac{\partial E_z(x,0,z)}{\partial x}\right)_{x=x_0} e^{ikz}dz\right|^2}{W\omega_0} = \frac{\omega_0^2}{\left(\omega^2 - \omega_0^2 - i\frac{\omega\omega_0}{Q}\right)} \times \left(\frac{x_0}{k}\right) I_0\left(\frac{r_\parallel}{Q}\right)$$

where $\quad \left(\frac{r_\parallel}{Q}\right) \equiv \dfrac{\left|\int_{-\infty}^{\infty}\left(\frac{\partial E_z(x,0,z)}{\partial x}\right)_{x=x_0} e^{ikz}dz\right|^2}{W\omega_0}$

is dipole longitudinal impedance. and $k = \omega_0/c$. **Dipole** $\left(\frac{r_\parallel}{Q}\right)$ **is measured in Ohm/m².**

Appendix 10:

RF-kick may be expressed through the transverse impedance:

$$U_{kick} = \frac{\omega_0^2}{\left(\omega^2 - \omega_0^2 - i\frac{\omega\omega_0}{Q}\right)} \times x_0 I_0 \left(\frac{r_\perp}{Q}\right),$$

where $\left(\frac{r_\perp}{Q}\right) \equiv \left(\frac{r_\parallel}{Q}\right) \times \frac{1}{k} = \dfrac{\left|\int_{-\infty}^{\infty} \left(\frac{\partial E_z(x,0,z)}{\partial x}\right)_{x=x_0} e^{ikz} dz\right|^2}{kW\omega_0}.$

Note that $\left(\dfrac{r_\perp}{Q}\right)$ is measured in <u>Ohm/m</u>.

At resonance

$$U_{kick} = i\left(\frac{x_0}{k}\right) I_0 Q \left(\frac{r_\parallel}{Q}\right) = ix_0 I_0 Q \left(\frac{r_\perp}{Q}\right).$$

🎇 **Fermilab**

Appendix 10:

Sometimes they use other transverse impedance, that is determined as:

$$\left(\frac{r_\perp}{Q}\right)_1 = \frac{|U_{kick}|^2}{\omega_0 W_0},$$

where W_0 is the energy, stored in the cavity at the RF field amplitude which provides given transverse kick U_{kick}, $W_0 = |A|^2 W$. At the resonance one has

$$|A|^2 = \frac{\left| x_0 I_0 Q \int_{-\infty}^{\infty} \left(\frac{\partial E_z(x,0,z)}{\partial x}\right)_{x=x_0} e^{ikz} dz \right|^2}{(W\omega_0)^2} = \left(\frac{r_\parallel}{Q}\right) \frac{(x_0 I_0 Q)^2}{W\omega_0}$$

and

$$\omega_0 W_0 = \omega_0 W |A|^2 = \left(\frac{r_\parallel}{Q}\right)(x_0 I_0 Q)^2 .$$ On the other hand, $\quad |U_{kick}|^2 = \frac{1}{k^2}\left(x_0 I_0 Q \left(\frac{r_\parallel}{Q}\right)\right)^2$

and

$$\left(\frac{r_\perp}{Q}\right)_1 = \frac{|U_{kick}|^2}{\omega_0 W_0} = \left(\frac{r_\parallel}{Q}\right) \times \frac{1}{k^2}.$$

$\left(\frac{r_\perp}{Q}\right)_1$ **is measured in <u>Ohm</u>.** Note that $\qquad U_{kick} = i(kx_0)I_0 Q \left(\frac{r_\perp}{Q}\right)_1$

✦ Fermilab

Appendix 11: Travelling–Wave acceleration structures:

- Each previous cell exits EM filed in a current cell, which in turn excites the field in the next cell.

- Pillbox cells with thin walls →
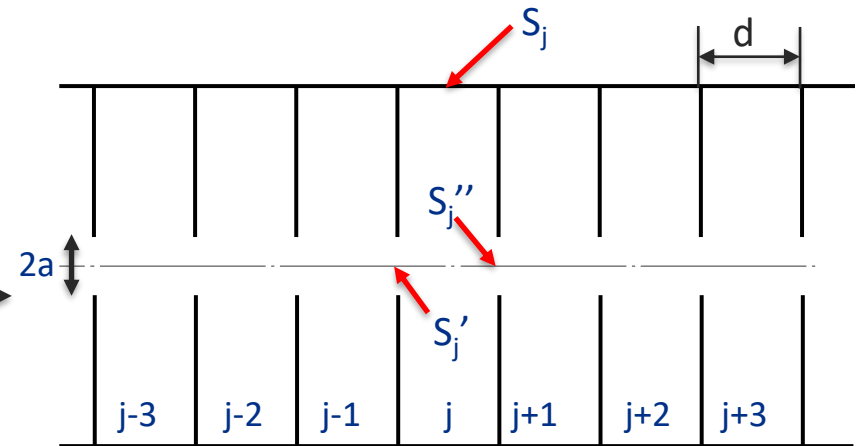
S_i is the cell metallic surface, S_j' and S_j'' are the coupling holes; V is the cell volume.

$\vec{E_j}, \vec{H_j}$ - fields in the jth pillbox cell oscillate at frequency ω;

$\vec{E}_{j,n}, \vec{H}_{j,n}$ - eigenmodes in the jth pillbox cell oscillate at frequency ω_n;

All the fields satisfy Maxwell Equations. Boundary conditions:

$\vec{E_j} \times n = 0$ on S_i; $\vec{E}_{j,n} \times n = 0$ on $S_i + S_j' + S_j''$.

Appendix 11: Travelling–Wave acceleration structures.

We consider the following:

$$\int_{V_j} \vec{\nabla} \cdot \left(\vec{E}_j \times \vec{H}_{j,n}^* \right) dV = \int_{V_j} [\vec{H}_{j,n}^* \cdot \left(\vec{\nabla} \times \vec{E}_j \right) - \vec{E}_j \cdot \left(\vec{\nabla} \times \vec{H}_{j,n}^* \right)] dV$$

$$= \int_{V_j} [-i\omega\mu_0 \vec{H}_j \cdot \vec{H}_{j,n}^* - i\omega_n\varepsilon_0 \cdot \vec{E}_{j,n}^* \cdot \vec{E}_j] dV$$

Using Gauss theorem and boundary conditions we have

$$\omega_n\varepsilon_0 \int_{V_j} \vec{E}_{j,n}^* \cdot \vec{E}_j \, dV - \omega\mu_0 \int_{V_j} \vec{H}_j \cdot \vec{H}_{j,n}^* \, dV = \frac{1}{i}\int_{S_j'+S_j''} (\vec{E}_j \times \vec{H}_{j,n}^*) \cdot dS \qquad (1)$$

Similarly, by considering

$$\int_{V_j} \vec{\nabla} \cdot \left(\vec{H}_j \times \vec{E}_{j,n}^* \right) dV$$

we have

$$\omega\varepsilon_0 \int_{V_j} \vec{E}_{j,n}^* \cdot \vec{E}_j \, dV - \omega_n\mu_0 \int_{V_j} \vec{H}_j \cdot \vec{H}_{j,n}^* \, dV = 0 \qquad (2)$$

The eigenmode expansion:

$$\vec{E}_j = \sum X_{j,n}\vec{E}_{j,n}$$

$$\vec{H}_j = \sum Y_{j,n}\vec{H}_{j,n}$$

🎴 Fermilab

Appendix 11: Travelling–Wave acceleration structures:

By using (1) and (2) we obtain

$$X_{j,n} = -\frac{i\omega_n}{\omega^2 - \omega_n^2} \cdot \frac{\int_{S_j' + S_j''}(\vec{E}_j \times \vec{H}_{j,n}^*) \cdot dS}{2W_{j,n}} \qquad (3)$$

$$Y_{j,n} = \frac{i\omega}{\omega^2 - \omega_n^2} \cdot \frac{\int_{S_j' + S_j''}(\vec{E}_j \times \vec{H}_{j,n}^*) \cdot dS}{2W_{j,n}}$$

The eigenmode amplitudes are determined by tangential electric field on the holes, E_{rj}

How to find E_{rj} for small holes?

1. Quasi-static approximation:

We have: $\Delta\vec{E}_j + k^2\vec{E}_j = 0$, $k^2 = \frac{\omega^2}{c^2}$

For a small hole, $a \ll \lambda_{..}$. It means that $\Delta\vec{E}_j \sim \frac{\vec{E}_j}{a^2} \gg k^2\vec{E}_j = \left(\frac{\omega}{c}\right)^2 \vec{E}_j$ and $\Delta\vec{E}_j \approx 0$

i.e., it means that $\vec{E}_j = \vec{\nabla}\Phi$, $\Delta\Phi = 0$ or electric field is quasi-static.

Far from the holes electric field has only longitudinal (accelerating) component!

Fermilab

Appendix 11: Travelling–Wave acceleration structures:

2. Superposition:
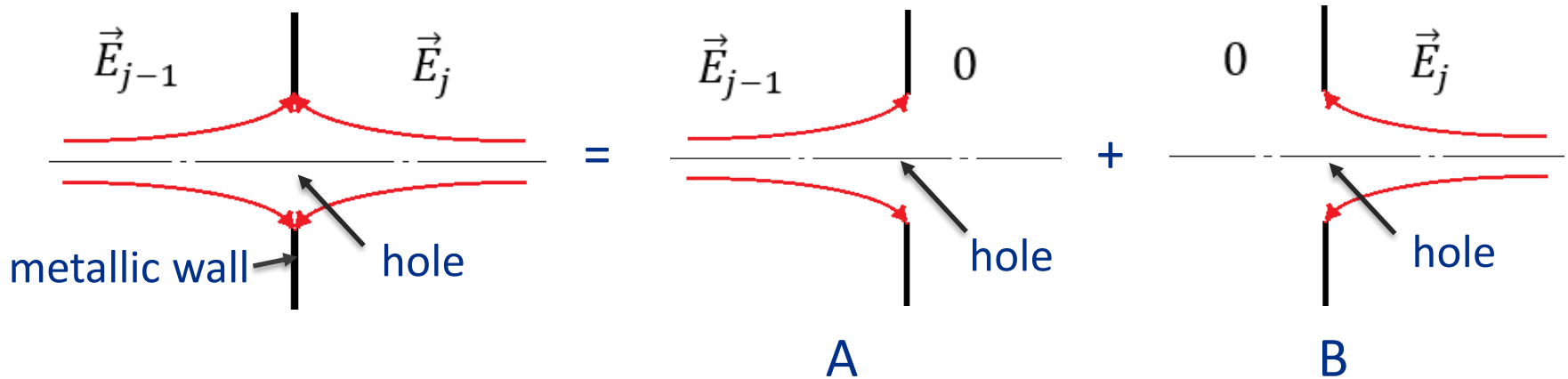
3. Electrostatic problem: conducting sheet at $z=0$ with a circular hole of the radius a, at $z=-\infty$ the field is homogeneous, $E_z=E_0$; at $z=\infty$ the field $E=0$: problem A above. The problem has analytical solution.*

We need to define the radial electric field at the hole, or at $z=0$.

* W.R. Smythe, Static and Dynamic Electricity, 1939, p. 159

🎝 **Fermilab**

Appendix 11: Travelling–Wave acceleration structures:

Oblate spheroidal coordinates:

$$\frac{z^2}{\zeta^2} + \frac{r^2}{1+\zeta^2} = a^2 \quad \text{spheroids}$$

$$-\frac{z^2}{\xi^2} + \frac{r^2}{1-\xi^2} = a^2 \quad \text{hyperboloids}$$

$$r = a[(1+\zeta^2)(1-\xi^2)]^{1/2}$$

$$z = a\zeta\xi$$

$$\Delta\Phi = 0$$

$$\Phi(\xi,\zeta) = aE_0\xi\left[\zeta - \frac{1}{\pi}(\zeta\cot^{-1}\zeta - 1)\right]$$

$$E_r(r,0) = \frac{1}{h_1}\nabla_\xi(\Phi(\xi,\zeta)|_{\zeta=0} = E_0\frac{(1-\xi^2)^{\frac{1}{2}}}{\pi\xi} = E_0\frac{r}{\pi(a^2-r^2)^{1/2}}$$

$$E_z(r,0) = \frac{1}{h_2}\nabla_\zeta(\Phi(\xi,\zeta)|_{\zeta=0} = \frac{1}{2}E_0$$
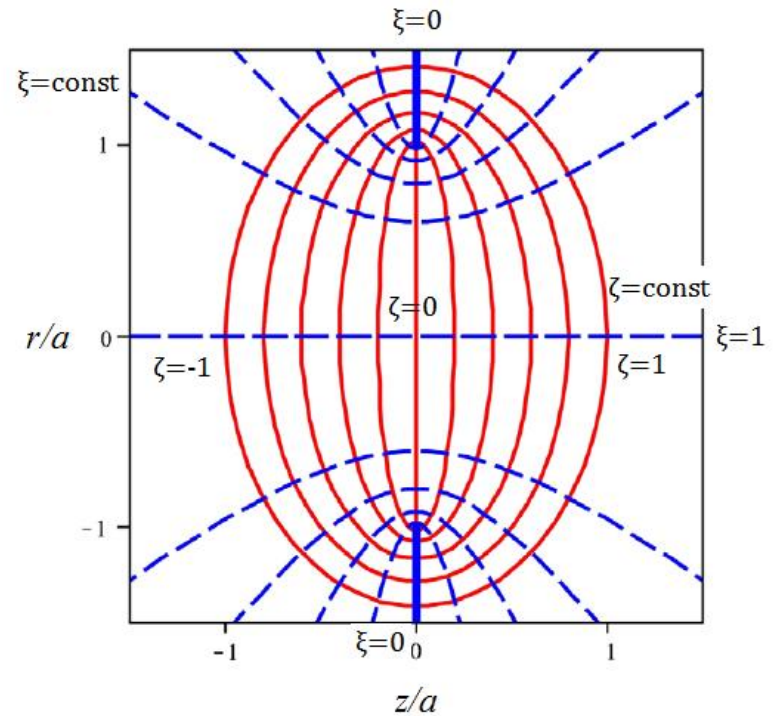
Lamet coefficients

$$h_1 = a\left(\frac{\xi^2-\zeta^2}{1-\xi^2}\right)^{1/2}$$

$$h_2 = a\left(\frac{\xi^2-\zeta^2}{1+\zeta^2}\right)^{1/2}$$

🔷 Fermilab

Appendix 11: Travelling–Wave acceleration structures:

For TM_{010} mode in a pillbox near the axis (see slide 32):

$$E_{j,r}(r)|_{S'_j} = E_0 \frac{r}{\pi(a^2 - r^2)^{1/2}} [X_{j-1} - X_j]$$

$$E_{j,r}(r)|_{S''_j} = E_0 \frac{r}{\pi(a^2 - r^2)^{1/2}} [X_j - X_{j+1}]$$

$$H_{j,\varphi}(r) \approx -iE_0 \frac{(\frac{\omega_0}{c})r}{2Z_0}$$

and from (3), slide 69, we have:

$$X_j \left[1 - (1 + K) \frac{\omega_0^2}{\omega^2} \right] + \frac{1}{2} K \frac{\omega_0^2}{\omega^2} [X_{j-1} + X_{j+1}] = 0 \qquad (1)$$

where K is the coupling, dimensionless parameter:

$$K = \frac{2E_0^2 a^3}{3Z_0 W_0 c} = \frac{2}{3} \cdot \frac{R/Q}{Z_0} \cdot \frac{k_0 a^3}{d^2 T^2} \qquad k_0 = \frac{\omega_0}{c}$$

$K \sim a^3$. For a thick wall $K \sim a^\eta$, $\eta > 3$ *(field decays in the coupling hole).*

🎇 **Fermilab**

Appendix 11: Travelling–Wave acceleration structures:

In the infinite chain of cavities equation (1) has solution (travelling wave):
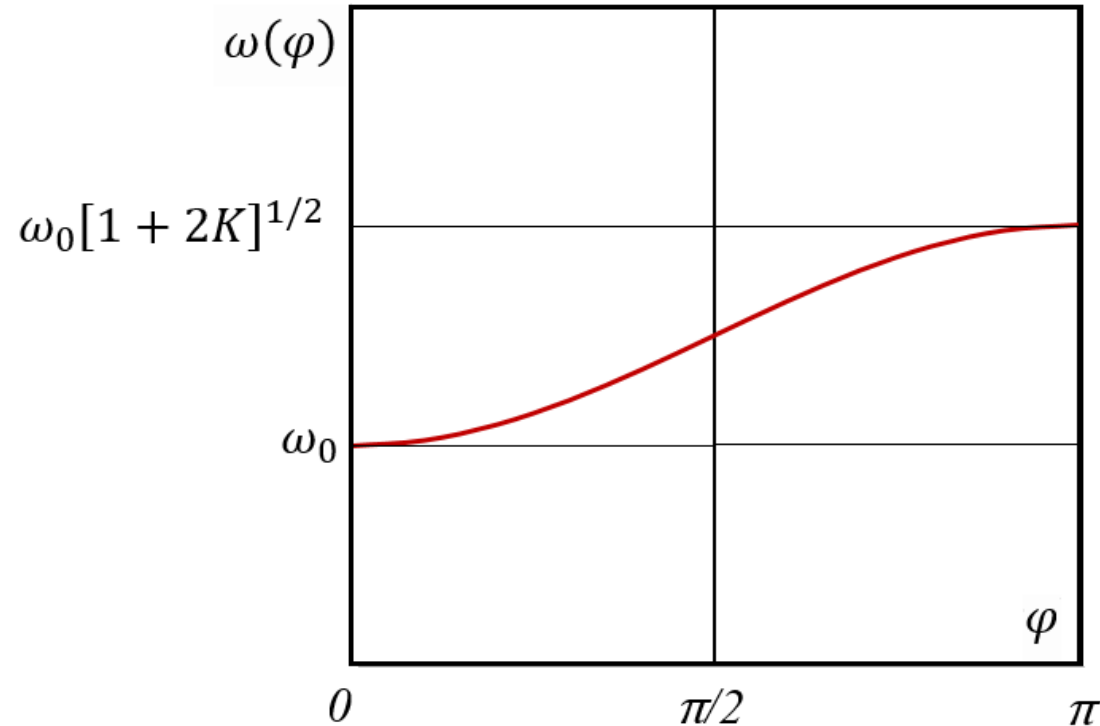
$$X_j = X e^{ij\varphi}$$

and

$$\omega(\varphi) = \omega_0 [1 + K(1 - cos\varphi)]^{1/2}$$

For small K we have:

$$\omega(\varphi) \approx \omega_0 [1 + \tfrac{1}{2} K(1 - cos\varphi)]$$

One can see that

$$K = \frac{\omega(\pi) - \omega(0)}{\omega(0)}$$

🎣 **Fermilab**

Appendix 11: Travelling–Wave acceleration structures. The 2d Bell theorem, illustration:

For a pillbox structure:

The fields on the hole are equal to

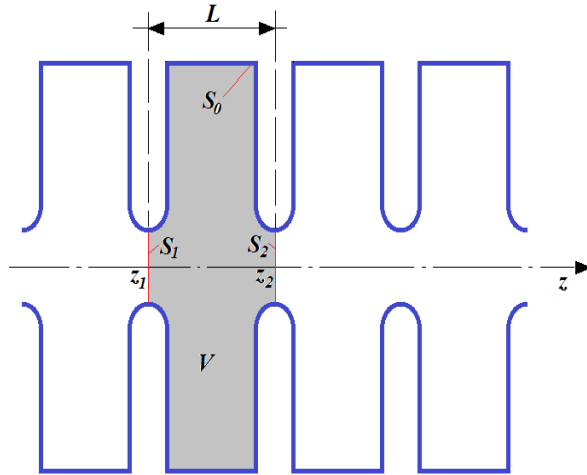$$E_{j,r}(r)|_{S_j'} = E_0 \frac{r}{\pi(a^2 - r^2)^{1/2}} [X_{j-1} - X_j]$$

$$H_{j,\varphi}(r)|_{S_j'} \approx -iE_0 \frac{\left(\frac{\omega_0}{c}\right) r}{4Z_0} [X_{j-1} + X_j]$$

(E_z and H_ϕ on the hole are two times smaller than in the cell center, see slides 71-72).

Therefore, we have

$$v_{gr} = \frac{P}{\frac{|X_j|^2 W_0}{d}} = \frac{\frac{1}{2}Re \int E_r H_\varphi^* dS}{\frac{|X_j|^2 W_0}{d}} = \frac{\omega_0 E_0^2 a^3 d}{6Z_0 W_0 c} Re\left[i(X_{j-1} - X_j)(X_{j-1}^* + X_j^*)\right] =$$

$$= \frac{\omega_0 E_0^2 a^3 d}{3Z_0 W_0 c} \sin(\varphi) = \frac{\omega_0 d}{2} K\sin(\varphi) = c\frac{\pi K d}{\lambda} \sin(\varphi) = \frac{d\omega}{dk_z}$$

🟠 **Fermilab**

Bell theorems for periodic acceleration structures, proof

I. Floquet Theorem

"For a given mode of propagation in a periodic system at given steady-state frequency the fields at one cross section differ from that one period away only by complex constant".

$$\vec{E}(x, y, z_2) = \vec{E}(x, y, z_1)e^{-ik_zL}$$
$$\vec{H}(x, y, z_2) = \vec{H}(x, y, z_1)e^{-ik_zL} \qquad (1)$$
$$z_2 = z_1 + L$$

II. 1st Bell Theorem

"The time-average electrical stored energy per period is equal to the time-average magnetic stored energy per period in the passband".

Consider the periodic structure to be divided by a series of surfaces perpendicular to the axis spaced by the periodic distance L. One cell of the structure having the volume V is surrounded by these surfaces S_1 and S_2 and the ideal metal boundary S_0. Let's consider the integral over the surface surrounding the cell, which equals to zero:

$$\oint \vec{E} \times \vec{H}^* \cdot d\vec{s} = \int_{S_0} \vec{E} \times \vec{H}^* \cdot d\vec{s} + \int_{S_1} \vec{E} \times \vec{H}^* \cdot d\vec{s} + \int_{S_2} \vec{E} \times \vec{H}^* \cdot d\vec{s} = 0 \qquad (2)$$

This is because we have

$$\int_{S_0} \vec{E} \times \vec{H}^* \cdot d\vec{s} = 0 \text{ because } E_t = 0 \text{ on } S_0$$

and $\int_{S_1} \vec{E} \times \vec{H}^* \cdot d\vec{s} + \int_{S_2} \vec{E} \times \vec{H}^* \cdot d\vec{s} = 0$ because of (1) and $d\vec{s}_2 = -d\vec{s}_1$

Fermilab

Bell theorems for periodic acceleration structures, proof

From Maxwell equations

$$rot\vec{E} = -i\omega\mu_0\vec{H} \qquad\qquad (3)$$
$$rot\vec{E}^* = i\omega\mu_0\vec{H}^*$$

and (2) we have

$$\oint \vec{E} \times rot\vec{E}^* \cdot d\vec{s} = 0$$

Applying Gauss's theorem, we get:

$$\int_V div(\vec{E} \times rot\vec{E}^*)dv = 0 . \qquad\qquad (4)$$

Using the vector theorem (see Appendix 1)

$$div(\vec{A} \times \vec{B}) = \vec{B} \cdot rot\vec{A} - \vec{A} \cdot rot\vec{B}, \qquad\qquad (5)$$

we get:

$$\int_V (rot\vec{E}^*) \cdot (rot\vec{E})dv - \int_V \vec{E} \cdot (rot(rot\vec{E}^*))dv = 0 .$$

Using Maxwell's equations (3) and the homogenous wave equation derived therefrom (see Lecture 1)

$$rot(rot\vec{E}^*)) = \omega^2\mu_0\varepsilon_0\vec{E}^* \qquad\qquad (6)$$

we get

$$\int_V (-i\omega\mu_0\vec{H}) \cdot (i\omega\mu_0\vec{H}^*)dv - \int_V \vec{E} \cdot (\omega^2\mu_0\varepsilon_0\vec{E}^*)dv = 0$$

Dividing through $4\omega^2\mu_0$ yields:

$$\boxed{\frac{1}{4}\int_V \mu_0|\vec{H}|^2 dv = \frac{1}{4}\int_V \varepsilon_0|E|^2 dv = W/2,}$$

quod erat demonstrandum.

Here W is total energy of electromagnetic field per period,

$$W = \frac{1}{2}\int_V \varepsilon_0\vec{E} \cdot \vec{E}^* dv = \frac{1}{2}\int_V \mu_0\vec{H} \cdot \vec{H}^* dv$$

☰ Fermilab

Bell theorems for periodic acceleration structures, proof

III. 2^d Bell Theorem

"The time-average power flow in the pass band is equal to the group velocity times time-average electro-magnetic stored energy per period divided by the period."

Consider (4) wherein $\vec{E}$ and $\vec{E}^*$ are functions of frequency ω. Differentiate with respect to frequency:

$$\frac{\partial}{\partial \omega} \int_V div(\vec{E} \times rot\vec{E}^*)dv = 0.$$

It gives:

$$\int_V div\left(\frac{\partial \vec{E}}{\partial \omega} \times rot\vec{E}^*\right)dv + \int_V div\left(\vec{E} \times rot\frac{\partial \vec{E}^*}{\partial \omega}\right)dv = 0.$$

Using the vector identity equation (5), we get

$$\int_V (rot\vec{E}^*) \cdot \left(rot\frac{\partial \vec{E}}{\partial \omega}\right)dv - \int_V \frac{\partial \vec{E}}{\partial \omega} \cdot (rot(rot\vec{E}^*))dv + .$$

$$+\int_V (rot\vec{E}) \cdot \left(rot\frac{\partial \vec{E}^*}{\partial \omega}\right)dv - \int_V \vec{E} \cdot \left(rot(rot\frac{\partial \vec{E}^*}{\partial \omega})\right)dv = 0 (7)$$

Differentiation (6) with respect to ω gives

$$rot(rot\frac{\partial \vec{E}^*}{\partial \omega})) = 2\omega\mu_0\varepsilon_0\vec{E}^* + \omega^2\mu_0\varepsilon_0\frac{\partial \vec{E}^*}{\partial \omega}$$

Using this in the second and fourth integrals of (7)

$$\int_V (rot\vec{E}^*) \cdot \left(rot\frac{\partial \vec{E}}{\partial \omega}\right)dv - \omega^2\mu_0\varepsilon_0\int_V \frac{\partial \vec{E}}{\partial \omega} \cdot \vec{E}^*dv +$$

$$+ \int_V (rot\vec{E}) \cdot \left(rot\frac{\partial \vec{E}^*}{\partial \omega}\right)dv - 2\omega\mu_0\varepsilon_0\int_V \vec{E} \cdot \vec{E}^*dv - \omega^2\mu_0\varepsilon_0\int_V \frac{\partial \vec{E}^*}{\partial \omega}\vec{E} \cdot dv = 0$$

which is

$$2Re\left\{\int_V (rot\vec{E}^*) \cdot \left(rot\frac{\partial \vec{E}}{\partial \omega}\right)dv - \int_V \frac{\partial \vec{E}}{\partial \omega} \cdot (rot(rot\vec{E}^*))dv\right\} - 2\omega\mu_0\varepsilon_0\int_V \vec{E} \cdot \vec{E}^*dv = 0.$$

🔷 **Fermilab**

Bell theorems for periodic acceleration structures, proof

Using (5) in reverse,

$$2Re\left\{\int_V \, div\left(\frac{\partial \vec{E}}{\partial \omega} \times rot\vec{E}^*\right)dv\right\} - 2\omega\mu_0\varepsilon_0 \int_V \, \vec{E}\cdot\vec{E}^* dv = 0.$$

and using Gauss's theorem on the first term,

$$2Re\left\{\oint \frac{\partial \vec{E}}{\partial \omega} \times rot\vec{E}^* \cdot d\vec{s}\right\} - 2\omega\mu_0\varepsilon_0 \int_V \, \vec{E}\cdot\vec{E}^* dv = 0. \qquad (8)$$

Integral $\int_{S_0} \frac{\partial \vec{E}}{\partial \omega} \times rot\vec{E}^* \cdot d\vec{s} = 0$ because of boundary conditions on the ideal metal surface.

From Floquet theorem (1) the following relation hold:

$$\vec{E}(x,y,z_2) = \vec{E}(x,y,z_1)e^{-ik_zL}$$

$$rot\vec{E}^*(x,y,z)|_{z=z_2} = rot\vec{E}^*(x,y,z)|_{z=z_1}e^{ik_zL} \qquad (9)$$

$$\vec{E}^*(x,y,z_2) = \vec{E}^*(x,y,z_1)e^{ik_zL}$$

$$\frac{\partial \vec{E}(x,y,z_2)}{\partial \omega} = \frac{\partial \vec{E}(x,y,z_1)}{\partial \omega}e^{-ik_zL} - iL\frac{dk_z}{d\omega}\vec{E}(x,y,z_1)e^{-ik_zL}$$

Separating the surface integral of (8)

$$2Re\left\{\int_{S_1} \frac{\partial \vec{E}(x,y,z_1)}{\partial \omega} \times rot\vec{E}^*(x,y,z)|_{z=z_1} \cdot d\vec{s} + \int_{S_2} \frac{\partial \vec{E}(x,y,z_2)}{\partial \omega} \times rot\vec{E}^*(x,y,z)|_{z=z_2} \cdot d\vec{s}\right\} -$$

$$2\omega\mu_0\varepsilon_0 \int_V \, \vec{E}\cdot\vec{E}^* dv = 0$$

and substituting equations (9)

$$2Re\left\{\int_{S_1} \frac{\partial \vec{E}(x,y,z_1)}{\partial \omega} \times rot\vec{E}^*(x,y,z)|_{z=z_1} \cdot d\vec{s} + \right.$$

$$\left. \int_{S_2} \frac{\partial \vec{E}(x,y,z_1)}{\partial \omega} \times rot\vec{E}^*(x,y,z)|_{z=z_1} \cdot d\vec{s} - iL\frac{dk_z}{d\omega}\int_{S_2} \vec{E}(x,y,z_1) \times rot\vec{E}^*(x,y,z)|_{z=z_1} \cdot d\vec{s}\right\} -$$

$$2\omega\mu_0\varepsilon_0 \int_V \, \vec{E}\cdot\vec{E}^* dv = 0$$

Fermilab

Bell theorems for periodic acceleration structures, proof

Since $d\vec{s}_2 = -d\vec{s}_1$ the first two integrals cancel. Using Maxwell equation (3) and condition s (9) we get

$$2Re\left\{\omega\mu_0 L \frac{dk_z}{d\omega}\int_{S_2}\vec{E}(x,y,z_2)\times\vec{H}^*(x,y,z_2)\cdot d\vec{s}\right\} - 2\omega\mu_0\varepsilon_0\int_V \vec{E}\cdot\vec{E}^*dv = 0$$

Multiplying by $\dfrac{1}{4\omega\mu_0 L}\dfrac{d\omega}{dk_z}$ we finally have

$$\frac{1}{2}Re\left\{\int_{S_2}\vec{E}(x,y,z_2)\times\vec{H}^*(x,y,z_2)\cdot d\vec{s}\right\} = \frac{d\omega}{dk_z}\cdot\frac{1}{L}\cdot\frac{1}{2}\int_V \varepsilon_0\vec{E}\cdot\vec{E}^*dv = 0$$

or

$$\boxed{P = v_{gr}w,}$$

here

$P = \dfrac{1}{2}Re\left\{\int_{S_2}\vec{E}(x,y,z_2)\times\vec{H}^*(x,y,z_2)\cdot d\vec{s}\right\}$ is the time averaged power flaw in the passbands;

$v_{gr} = \dfrac{d\omega}{dk_z}$ is a group velocity;

$w = \dfrac{1}{L}\cdot\dfrac{1}{2}\int_V \varepsilon_0\vec{E}\cdot\vec{E}^*dv = \dfrac{1}{L}\cdot\dfrac{1}{2}\int_V \mu_0\vec{H}\cdot\vec{H}^*dv = \dfrac{W}{L}$ is the time-averaged stored electromagnetic energy per unit length.

[1] J.S. Bell, "Group velocity and energy velocity in periodic waveguides," Harwell, AERE-T-R-858 (1952)
[2] D.A. Watkins, Topics in Electromagnetic Theory, John Willey & Sons, Inc. London, 1958
[3] E. A. *Burshtein*, and G. B. *Voskresensky*, The Intensive Beam Electron Linear Accelerators, Atomizdat, Moscow, 1970.

‡ Fermilab

Appendix 12: Standing –Wave acceleration structures. Perturbation theory.

In matrix form Eq(1), see Lecture 2, Slide 44:

$$M\hat{X} - \frac{\omega_0^2}{\omega^2}\hat{X} = 0$$

here $\quad M_{jj} = 1; \ j = 0,1,\dots N;$

$$M_{jj-1} = \frac{K}{2W(j)}; \ j = 1,2,\dots N; \ M_{jj+1} = \frac{K}{2W(j)}; j = 0,1,\dots N-1.$$

and $\quad W(j) = 1, j = 1,2,\dots N-1 \quad W(j) = \frac{1}{2}, j = 0, N$

Eigenvectors and eigenvalues:

$$\hat{X}_j^q = \cos\frac{\pi q j}{N}; \ \omega_q^2 = \frac{\omega_0^2}{1 + K\cos\frac{\pi q}{N}}, q = 0,1,\dots N$$

Orthogonality:

$$\hat{X}^q \cdot \hat{X}^r \equiv \sum_{j=0}^{N} W(j)\,\hat{X}_j^q \hat{X}_j^r = \frac{N\delta_{qr}}{2W(q)}, \quad \delta_{qq} = 1, and \ \delta_{qr} = 0, if \ q \neq r$$

🎺 **Fermilab**

Appendix 12: Standing –Wave acceleration structures. Perturbation theory

- Perturbation of the cell resonance frequencies causes perturbation of the mode resonance frequencies $\delta\omega_q$;
- the field distribution $\delta\hat{X}_q$.

$$\omega_{0j}^{2\prime} = \omega_0^2 + \delta\omega_{0j}^2 \quad \rightarrow \hat{X}^{q\prime} = \hat{X}^q + \delta\hat{X}^q, \quad \hat{X}^q \cdot \delta\hat{X}^q$$

Variation of the equation (1), see previous

slide, gives $M\delta\hat{X}^q = \dfrac{\omega_0^2}{\omega_q^2}\left[\delta\hat{X}^q + \Omega\hat{X}^q - \dfrac{\delta\omega_q^2}{\omega_q^2}\hat{X}^q\right],$ where $\Omega = \begin{bmatrix} \dfrac{\delta\omega_{01}^2}{\omega_0^2} & \cdots & 0 \\ \vdots & \ddots & \vdots \\ 0 & \cdots & \dfrac{\delta\omega_{0N}^2}{\omega_0^2} \end{bmatrix}$

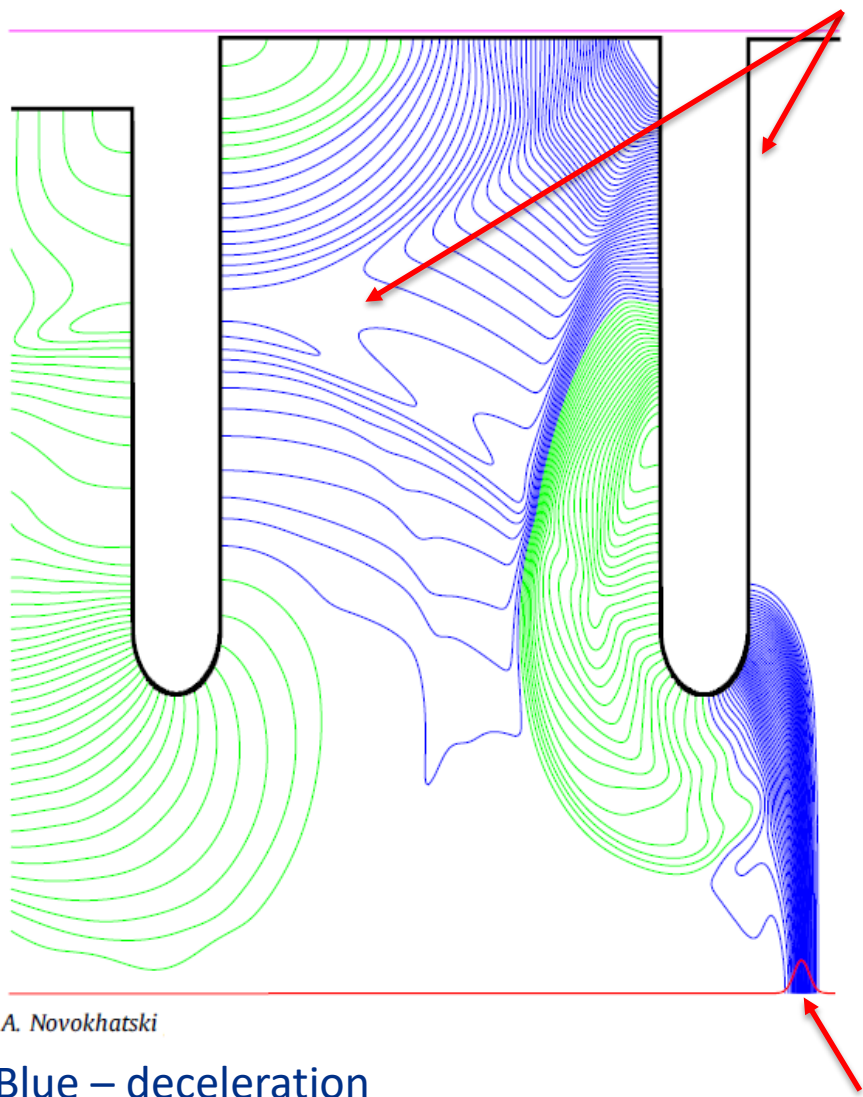$$\frac{\delta\omega_q^2}{\omega_q^2} = [2W(q)/N]\cdot\hat{X}^q\Omega\hat{X}^q;$$

$$\delta\hat{X}^q = \sum_{q\prime\neq q}\frac{2W(q\prime)\hat{X}^q\Omega\hat{X}^q}{N\left(\dfrac{\omega_q^2}{\omega_{q\prime}^2}-1\right)}\hat{X}^{q\prime}$$

$$\left|\delta\hat{X}^q\right|\sim\frac{\left|\delta\omega_{0j}\right|_{av}}{\left|\omega_q-\omega_{q\pm1}\right|}$$

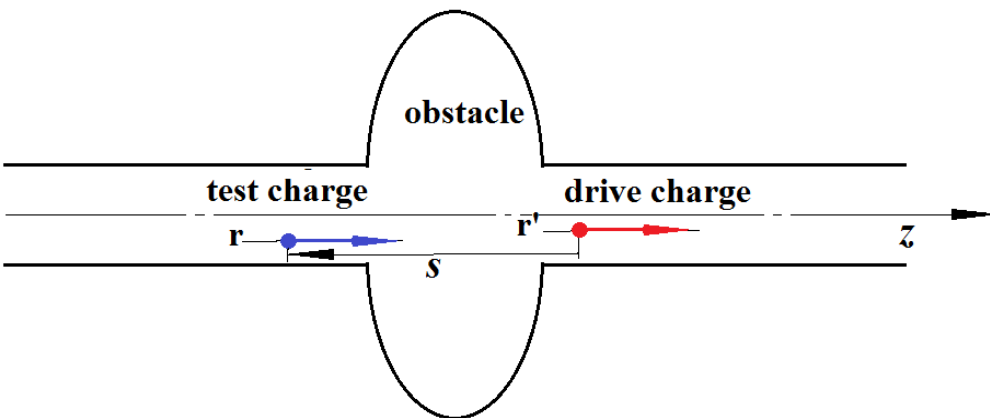**꜅ Fermilab**

Appendix 13: Wake potentials

Acceleration cells

Radiation fields in the
TW acceleration structure

A. Novokhatski

Blue – deceleration
Green - acceleration

bunch

$$W_z(\vec{r}, \vec{r}', s) = -\frac{1}{q} \int_{z_1}^{z_2} dz \, [E_z(\vec{r}, z, t)]_{t=(z+s)/c} \ ,$$

$$\overrightarrow{W}_\perp(\vec{r}, \vec{r}', s) = \frac{1}{q} \int_{z_1}^{z_2} dz \, \left[\vec{E}_\perp + c(\hat{z} \times \vec{B})\right]_{t=(z+s)/c} \ .$$

$W_z = 0, \ W_\perp = 0 \ for \ s < 0$

Fermilab

Appendix 13: Wake potentials

Loss and kick distribution along the bunch $V_z(s)$ and $V_\perp(s)$:

$$V_z(s) = \int_0^\infty ds' \, \lambda(s-s') \, W_z(s') = \int_{-\infty}^s ds' \, \lambda(s') \, W_z(s-s'),$$

$$\vec{V}_\perp(s) = \int_0^\infty ds' \, \lambda(s-s') \, \vec{W}_\perp(s') = \int_{-\infty}^s ds' \, \lambda(s') \, \vec{W}_\perp(s-s').$$

$\lambda(s)$ is the charge distribution along the bunch.

Total losses and kick:

$$\Delta U = \int_{-\infty}^\infty ds \, \lambda(s) \, V_z(s), \quad k_\ell = \frac{\Delta U}{q^2} \equiv \frac{1}{q^2} \int_{-\infty}^\infty ds \, \lambda(s) \, V_z(s) \qquad k_l - \text{loss factor}$$

$$k_{HOM} = k_l - \frac{1}{4} R/Q \cdot \omega|_{acc.\ mode}$$

$$\vec{p}_\perp = q^2 \vec{k}_\perp/c \qquad \vec{k}_\perp \equiv \frac{1}{q^2} \int_{-\infty}^\infty ds \, \lambda(s) \, \vec{V}_\perp(s) \qquad \vec{k}_\perp - \text{kick factor}$$

🟦 **Fermilab**

Appendix 13: Wake potentials

Panofsky-Wenzel theorem for wakes:

$$\frac{\partial \vec{W}_\perp}{\partial s} = \frac{c}{eq} \frac{\partial \vec{p}_\perp}{\partial s} = -\frac{1}{q} \int_0^L dz \left[\vec{\nabla}_\perp E_z(z,t) \right]_{t=(s+z)/c} = \vec{\nabla}_\perp W_z .$$

Relation between wake and impedance:

$$Z(\omega) = \int_0^\infty W_z(\tau) \exp\{-i\omega\tau\} \, d\tau \equiv \widetilde{W}_z(\tau) ,$$

$$s = c\tau = ct - z$$

$$Z(k) = \int_0^\infty W_z(s) \exp\{-iks\} \, ds \equiv \widetilde{W}_z(s) = c \left[Z(\omega) \right]_{\omega=kc}$$

and

$$k_\ell = \frac{\Delta U}{q^2} = \frac{1}{\pi q^2} \int_0^\infty Z_R(\omega) \, I^2(\omega) \, d\omega .$$

Fermilab